Statistical mechanics of neocortical interactions: Columnar EEG

Lester Ingber

Lester Ingber Research
Ashland Oregon USA
ingber@ingber.com, ingber@alumni.caltech.edu
http://www.ingber.com/

ABSTRACT: It is demonstrated that local columnar firings of neocortex, as modeled by a Statistical Mechanics of Neocortical Interactions (SMNI), supports multiple firing regions of multiple oscillatory processing, at frequencies consistent with observed regional electroencephalography (EEG). Direct calculations of the Euler-Lagrange (EL) equations which are derived from functional variation of the SMNI probability distribution, giving most likely states of the system, are performed for three prototypical cases, predominately excitatory columnar firings, predominately inhibitory columnar firings, and in between balanced columnar firings, with and without a centering mechanism (based on observed changes in stochastic background of presynaptic interactions) which pulls more stable states into the physical firings ranges. These calculations are repeated for the visual neocortex, which has twice as many neurons/minicolumn as other neocortical regions. The nonlinearities lead to very long codes and here the results are presented as graphs over the firing space.

KEYWORDS: EEG; short term memory; nonlinear; statistical

1. Introduction to Origins of EEG

The origins and utility of observed electroencephalography (EEG) are not yet clear. That is, many neuroscientists believe that global regional activity supports such wave-like oscillatory observations at various frequencies, e.g., popularly designated as alpha, beta, theta, etc (Nunez, 1974; Nunez, 1981; Nunez, 1995). Here, regional refers to major neocortical regions, e.g., visual, auditory, somatic, associative, frontal, etc. Global refers to interactions among these regions.

Some other investigators have shown how reasonable models of relatively local columnar activity can support oscillatory interactions (Ingber, 1983; Ingber, 1985b). Here, local refers to scales of interactions among neurons across columns consisting of hundreds of neurons and macrocolumns consisting of thousands of minicolumns. This local approach, using a Statistical Mechanics of Neocortical Interactions (SMNI) has also included global regional interactions among distant local columnar activity (Ingber & Nunez, 1990). SMNI has also demonstrated how most likely states described by multivariate probability distributions nonlinear in their means and covariances, i.e., as calculated as Euler-Lagrange (EL) equations directly from the SMNI Lagrangian. This Lagrangian is the argument in the exponent of the SMNI probability distribution. The EL equations are developed from a variational principle applied to this distribution, and they give rise to a nonlinear string model used by most neuroscientists to describe global oscillatory activity (Ingber, 1995a).

Just as a quantum string theory of neocortex might some day describe global neocortical activity, albeit unlikely, it still is not appropriate or useful to discuss aspects of measured neocortical EEG. Similarly, a molecular theory of weather over continents on Earth is not appropriate or useful to forecast daily weather patterns. Beyond criteria of being appropriate or useful, Nature has developed structures at intermediate scales in many biological as well as in many non-biological systems to facilitate flows of information between relatively small and large scales of activity. This has been discussed in the SMNI papers with respect to the development of columnar physiology in neocortex, which can be described by a nonlinear nonequilibrium multivariate statistical mechanics, a subfield of statistical mechanics dealing with Gaussian Markovian systems with time-dependent drifts and correlated diffusions, with both drifts and diffusions nonlinear in their multiple variables. Many systems possess such structures at so-called mesoscopic scales, intermediate between microscopic and macroscopic scales, where these scales are typically defined specific to each system, and where the mesoscopic scale typically facilitates information between the microscopic and macroscopic scales. Typically, these mesoscopic scales have their own interesting dynamics. SMNI has described columnar activity to be an effective mesoscopic scale intermediate between macroscopic regional interactions and microscopic averaged synaptic and neuronal interactions.

In this context, while EEG may have generators at microscopic neuronal scales and regional macroscopic scales, this study was motivated to investigate whether mesoscopic scales can support columnar firing activity at observed multiple frequencies, e.g., alpha, beta, theta, not necessarily generate such frequencies. The short answer is yes. The detailed support of this result requires quite lengthy calculations of the highly nonlinear multivariate SMNI system. However, a graphical presentation of the multivariate EL equations presents an accurate as well as intuitive depiction of these results, yielding equations of graphs, instead of the nonlinear multivariate algebra, or instead of the computer code generated by these equations (some of which are hundreds of thousands of lines long).

More recent work has developed this project using the full nonlinear EL equations, requiring use of the authors Adaptive Simulated Annealing (ASA) global sampling algorithm (Ingber, 2009).

Section 2 is a review of the SMNI model.

Section 3 presents calculations of the EL equations, which are based on direct calculations of the nonlinear multivariate EL equations of the SMNI Lagrangian, giving most likely states of the system, performed for three prototypical cases, predominately excitatory columnar firings, predominately inhibitory columnar firings, and in between balanced columnar firings, with and without a centering mechanism turned on which pulls more stable states into the physical firings ranges. This centering mechanism expresses experimentally observed changes in stochastic background of presynaptic interactions during selective attention. These calculations are repeated for the visual neocortex, which has twice as many neurons/minicolumn as other neocortical regions.

Section 4 takes an opportunity here to identify and correct a $\sqrt{2}$ error in the original SMNI work which has been propagated in over 30 papers up until now. This error does not affect any conclusions of previous results, but it must be corrected. Direct comparisons are made using EL results, which also presents an opportunity to see how robust the SMNI model is with respect to changes in synaptic parameters within their experimentally observed ranges.

Section 5 presents calculations of oscillatory states. Given the EL calculations, investigations are performed for each of the prototypical cases to see if and where oscillatory behavior is observed within experimentally observed ranges. These results also are presented graphically.

Section 6 is the conclusion, offering some conjecture on the utility of having columnar activity support oscillatory frequencies observed over regions of neocortex, e.g., to support conveying local neuronal information across regions as is observed in normal human activity.

2. Statistical Mechanics of Neocortical Interactions (SMNI)

Neocortex has evolved to use minicolumns of neurons interacting via short-ranged interactions in macrocolumns, and interacting via long-ranged interactions across regions of macrocolumns. This common architecture processes patterns of information within and among different regions of sensory, motor, associative cortex, etc.

2.1. SMNI Tests on Short-Term Memory and EEG

The author has developed a statistical mechanics of neocortical interactions (SMNI) for human neocortex, building from synaptic interactions to minicolumnar, macrocolumnar, and regional interactions in neocortex. Since 1981, a series of papers on the statistical mechanics of neocortical interactions (SMNI) has been developed to model columns and regions of neocortex, spanning mm to cm of tissue, As depicted in Figure 1, SMNI develops three biophysical scales of neocortical interactions: (a)-(a*)-(a') microscopic neurons; (b)-(b') mesocolumnar domains; (c)-(c') macroscopic regions. SMNI has developed conditional probability distributions at each level, aggregating up from the smallest levels of interactions. In (a*) synaptic inter-neuronal interactions, averaged over by mesocolumns, are phenomenologically described by the mean and variance of a distribution Ψ. Similarly, in (a) intraneuronal transmissions are phenomenologically described by the mean and variance of Γ. Mesocolumnar averaged excitatory (E) and inhibitory (I) neuronal firings M are represented in (a'). In (b) the vertical organization of minicolumns is sketched together with their horizontal stratification, yielding a physiological entity, the mesocolumn. In (b') the overlap of interacting mesocolumns at locations r and r' from times t and $t + \tau$ is sketched. In (c) macroscopic regions of neocortex are depicted as arising from many mesocolumnar domains. (c') sketches how regions may be coupled by long–ranged interactions.

Most of these papers have dealt explicitly with calculating properties of short-term memory (STM) and scalp EEG in order to test the basic formulation of this approach (Ingber, 1981; Ingber, 1982; Ingber, 1983; Ingber, 1984; Ingber, 1985b; Ingber, 1985c; Ingber, 1986b; Ingber & Nunez, 1990; Ingber, 1991; Ingber, 1992; Ingber, 1994; Ingber & Nunez, 1995; Ingber, 1995a; Ingber, 1995b; Ingber, 1996b; Ingber, 1996a; Ingber, 1997; Ingber, 1998). The SMNI modeling of local mesocolumnar interactions (convergence and divergence between minicolumnar and macrocolumnar interactions) was tested on STM phenomena. The SMNI modeling of macrocolumnar interactions across regions was tested on EEG phenomena.

The EEG studies in previous SMNI applications were focused on regional scales of interactions. The STM applications were focused on columnar scales of interactions. However, this EEG study is focused at columnar scales, and it is relevant to stress the successes of this SMNI at this columnar scale, giving support to this SMNI model in this context.

2.2. SMNI Description of STM

SMNI studies have detailed that maximal numbers of attractors lie within the physical firing space of M^G, where G = {Excitatory, Inhibitory} minicolumnar firings, consistent with experimentally observed capacities of auditory and visual STM, when a "centering" mechanism is enforced by shifting background
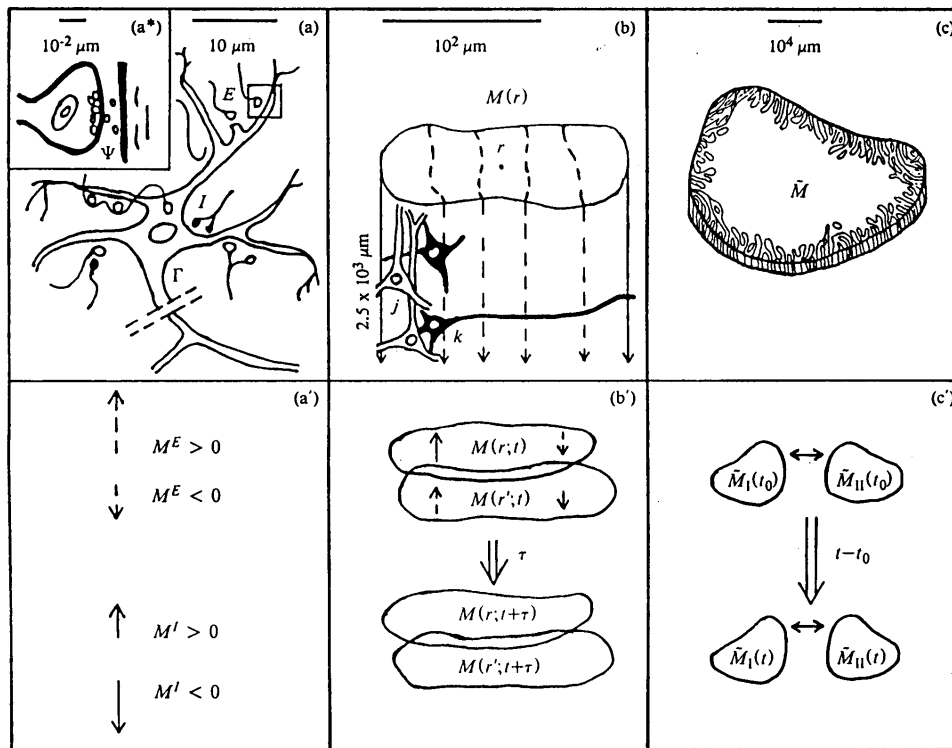
Fig. 1. Illustrated are three biophysical scales of neocortical interactions: (a)-(a*)-(a') microscopic neurons; (b)-(b') mesocolumnar domains; (c)-(c') macroscopic regions.

noise in synaptic interactions, consistent with experimental observations under conditions of selective attention (Mountcastle, Andersen & Motter, 1981; Ingber, 1984; Ingber, 1985c; Ingber, 1994; Ingber & Nunez, 1995). This leads to all attractors of the short-time distribution lying along a diagonal line in M^G space, effectively defining a narrow parabolic trough containing these most likely firing states. This essentially collapses the two-dimensional M^G space down to a one-dimensional space of most importance. Thus, the predominant physics of STM and of (short-fiber contribution to) EEG phenomena takes place in a narrow "parabolic trough" in M^G space, roughly along a diagonal line (Ingber, 1984).

These calculations were further supported by high-resolution evolution of the short-time conditional-probability propagator using PATHINT (Ingber & Nunez, 1995). SMNI correctly calculated the stability and duration of STM, the primacy versus recency rule, random access to memories within tenths of a second as observed, and the observed 7 ± 2 capacity rule of auditory memory and the observed 4 ± 2 capacity rule of visual memory.

SMNI also calculates how STM patterns (e.g., from a given region or even aggregated from multiple regions) may be encoded by dynamic modification of synaptic parameters (within experimentally observed ranges) into long-term memory patterns (LTM) (Ingber, 1983).

2.3. SMNI Description of EEG

Using the power of this formal structure, sets of EEG and evoked potential data from a separate NIH study, collected to investigate genetic predispositions to alcoholism, were fitted to an SMNI model on a lattice of regional electrodes to extract brain "signatures" of STM (Ingber, 1997; Ingber, 1998). Each electrode site was represented by an SMNI distribution of independent stochastic macrocolumnar-scaled M^G variables, interconnected by long-ranged circuitry with delays appropriate to long-fiber communication in neocortex. The global optimization algorithm Adaptive Simulated Annealing (ASA) (Ingber, 1989; Ingber, 1993a) was used to perform maximum likelihood fits of Lagrangians defined by path integrals of multivariate conditional probabilities. Canonical momenta indicators (CMI) were thereby derived for individual's EEG data. The CMI give better signal recognition than the raw data, and were used to advantage as correlates of behavioral states. In-sample data was used for training (Ingber,

1997), and out-of-sample data was used for testing (Ingber, 1998) these fits.

These results gave strong quantitative support for an accurate intuitive picture, portraying neocortical interactions as having common algebraic physics mechanisms that scale across quite disparate spatial scales and functional or behavioral phenomena, i.e., describing interactions among neurons, columns of neurons, and regional masses of neurons.

2.4. Generic Mesoscopic Neural Networks

SMNI was applied to a parallelized generic mesoscopic neural networks (MNN) (Ingber, 1992), as depicted in Figure 2, adding computational power to a similar paradigm proposed for target recognition (Ingber, 1985a).
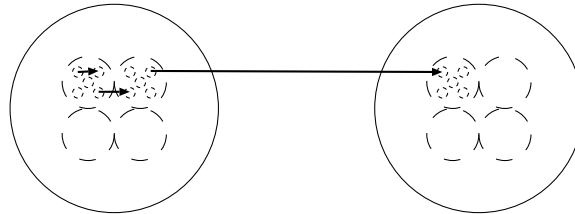
Fig. 2. Scales of interactions among minicolumns are represented, within macrocolumns, across macrocolumns, and across regions of macrocolumns.

"Learning" takes place by presenting the MNN with data, and parametrizing the data in terms of the firings, or multivariate firings. The "weights," or coefficients of functions of firings appearing in the drifts and diffusions, are fit to incoming data, considering the joint Lagrangian (including the logarithm of the prefactor in the probability distribution) as a dynamic cost function. This program of fitting coefficients in Lagrangian uses methods of ASA.

"Prediction" takes advantage of a mathematically equivalent representation of the Lagrangian path-integral algorithm, i.e., a set of coupled Langevin rate-equations. A coarse deterministic estimate to "predict" the evolution can be applied using the most probable path, but PATHINT has been used. PATHINT, even when parallelized, typically can be too slow for "predicting" evolution of these systems. However, PATHTREE is much faster.

2.5. ON Chaos in Neocortex

There are many papers on the possibility of chaos in neocortical interactions, including some that consider noise-induced interactions (Zhou & Kurths, 2003). While this phenomena may have some merit when dealing with small networks of neurons, e.g., in some circumstances such as epilepsy, these papers generally have considered only too simple models of neocortex.

The author took a model of chaos that might be measured by EEG, developed and published by colleagues (Nunez & Srinivasan, 1993; Srinivasan & Nunez, 1993), but adding background stochastic influences and parameters that were agreed to better model neocortical interactions. The resulting multivariate nonlinear conditional probability distribution was propagated many thousands of epochs, using the authors PATHINT code, to see if chaos could exist and persist under such a model (Ingber, Srinivasan & Nunez, 1996). There was absolutely no measurable instance of chaos surviving in this more realistic context. Again, note this study was at the columnar scale, not the finer scales of activity of smaller pools of neurons.

2.6. Mathematical Development

2.6.1. Background

A spatial-temporal lattice-field short-time conditional multiplicative-noise (nonlinear in drifts and diffusions) multivariate Gaussian-Markovian probability distribution is developed faithful to neocortical function/physiology. Such probability distributions are a basic input into the approach used here. The SMNI model was the first physical application of a nonlinear multivariate calculus developed by other

mathematical physicists in the late 1970's to define a statistical mechanics of multivariate nonlinear nonequilibrium systems (Graham, 1977; Langouche, Roekaerts & Tirapegui, 1982).

This formulation of a multivariate nonlinear nonequilibrium system required an excursion in a proper Riemannian geometry to study proper limits of short-time conditional probability distributions. Some tangible spin-offs from this study included applications to specific disciplines such as neuroscience (SMNI), finance (Ingber, 1990; Ingber, 2000), combat simulations (Ingber, 1993b), and nuclear physics (Ingber, 1986a) In addition there were generic computational tools developed, for optimization and importance-sampling with ASA (Ingber, 1993a), and for path-integral systems, including PATHINT (Ingber, 2000; Ingber & Nunez, 1995). and PATHTREE (Ingber, Chen, Mondescu *et al*, 2001).

2.6.2. Application to SMNI

Some of the algebra behind SMNI depicts variables and distributions that populate each representative macrocolumn in each region.

A derived mesoscopic Lagrangian L_M defines the short-time probability distribution P_M of firings in a minicolumn composed of $\sim 10^2$ neurons, by aggregating probability distributions of neuronal firings p_{σ_j}, given its just previous interactions with all other neurons in its macrocolumnar surround. G is used to represent excitatory (E) and inhibitory (I) contributions. $\bar{G}$ designates contributions from both E and I.

$$P_M = \prod_G P_M^G[M^G(r; t+\tau)|M^{\bar{G}}(r'; t)]$$

$$= \sum_{\sigma_j} \delta\left(\sum_{jE} \sigma_j - M^E(r; t+\tau)\right)\delta\left(\sum_{jI} \sigma_j - M^I(r; t+\tau)\right)\prod_j^N p_{\sigma_j}$$

$$\approx \prod_G (2\pi\tau g^{GG})^{-1/2} \exp(-N\tau \underline{L}_M^G) ,$$

$$P_M \approx (2\pi\tau)^{-1/2} g^{1/2} \exp(-N\tau \underline{L}_M) , \tag{1}$$

$$\underline{L}_M = \underline{L}_M^E + \underline{L}_M^I = (2N)^{-1}(\dot{M}^G - g^G)g_{GG'}(\dot{M}^{G'} - g^{G'}) + M^G J_G/(2N\tau) - \underline{V}' ,$$

$$\underline{V}' = \sum_G \underline{V}''_{G'}^G (\rho\nabla M^{G'})^2 ,$$

$$g^G = -\tau^{-1}(M^G + N^G \tanh F^G) , \quad g^{GG'} = (g_{GG'})^{-1} = \delta_G^{G'} \tau^{-1} N^G \operatorname{sech}^2 F^G , \quad g = \det(g_{GG'}) ,$$

$$F^G = \frac{(V^G - a_{G'}^{|G|}v_{G'}^{|G|}N^{G'} - \frac{1}{2}A_{G'}^{|G|}v_{G'}^{|G|}M^{G'})}{((\pi/2)[(v_{G'}^{|G|})^2 + (\phi_{G'}^{|G|})^2](a_{G'}^{|G|}N^{G'} + \frac{1}{2}A_{G'}^{|G|}M^{G'}))^{1/2}} , \quad a_{G'}^G = \frac{1}{2}A_{G'}^G + B_{G'}^G ,$$

where $A_{G'}^G$ and $B_{G'}^G$ are minicolumnar-averaged inter-neuronal synaptic efficacies, $v_{G'}^G$ and $\phi_{G'}^G$ are averaged means and variances of contributions to neuronal electric polarizations. $M^{G'}$ and $N^{G'}$ in F^G are afferent macrocolumnar firings, scaled to efferent minicolumnar firings by $N/N* \sim 10^{-3}$, where $N*$ is the number of neurons in a macrocolumn, $\sim 10^5$. Similarly, $A_G^{G'}$ and $B_G^{G'}$ have been scaled by $N*/N \sim 10^3$ to keep F^G invariant. $\underline{V}'$ are mesocolumnar nearest-neighbor interactions. J_G was used in early papers to model influences on minicolumnar firings from long-ranged fibers across regions, but later papers have integrated these long-ranged fibers into the above framework as described below.

It is interesting to note that the numerator of F^G contains information derived from presynaptic firing interactions. The location of most stable states of this SMNI system are highly dependent on the interactions presented in this numerator. The denominator of F^G contains information derived from postsynaptic neuromodular and electrical processing of these firings. The nonlinearities present in this denominator most dramatically affect the number and nature of stable states at scales zoomed in at magnifications of over a hundred times, representing neocortical processing of detailed information

within a sea of stochastic activity.

2.6.3. Three Prototypical Firing Cases

Three Cases of neuronal firings were considered in the first introduction of STM applications of SMNI (Ingber, 1984). Below is a short summary of these details. Note that while it suffices to define these Cases using F^G, the full Lagrangian and probability distribution, upon which the derivation of the EL equations are based, are themselves quite nonlinear functions of F^G, e.g., via hyperbolic trigonometric functions, etc.

Since STM duration is long relative to τ, stationary solutions of $\overline{L}$ can investigated to determine how many stable minima $\ll \bar{M}^G \gg$ may simultaneously exist within this duration. However, time-dependent folding of the full time-dependent probability distribution supports persistence of these stable states within SMNI calculations of observed decay rates of STM (Ingber & Nunez, 1995).

It is discovered that more minima of $\overline{L}$ are created, i.e., brought into the physical firing ranges, if the numerator of F^G contains terms only in $\bar{M}^G$, tending to center $\overline{L}$ about $\bar{M}^G = 0$. That is, B^G is modified such that the numerator of F^G is transformed to

$$F'^G = \frac{-\frac{1}{2} A_{G'}^{|G|} v_{G'}^{|G|} M^{G'}}{\left((\pi/2)[(v_{G'}^{|G|})^2 + (\phi_{G'}^{|G|})^2](a_{G'}^{'|G|} N^{G'} + \frac{1}{2} A_{G'}^{|G|} M^{G'})\right)^{1/2}} \ , a_{G'}'^G = \frac{1}{2} A_{G'}^G + B_{G'}'^G \ , \tag{2}$$

The most likely states of the "centered" systems lie along diagonals in M^G space, a line determined by the numerator of the threshold factor in F^E, essentially

$$A_E^E M^E - A_I^E M^I \approx 0 \ , \tag{3}$$

noting that in F^I $I - I$ connectivity is taken to be very small relative to other pairings, so that $(A_E^I M^E - A_I^I M^I)$ is typically small only for small M^E.

Of course, any mechanism producing more as well as deeper minima is statistically favored. However, this particular "Centering" mechanism has plausible support: $M^G(t + \tau) = 0$ is the state of afferent firing with highest statistical weight. I.e., there are more combinations of neuronal firings, $\sigma_j = \pm 1$, yielding this state than any other $M^G(t + \tau)$, e.g., $\sim 2^{N^G + 1/2}(\pi N^G)^{-1/2}$ relative to the states $M^G = \pm N^G$. Similarly, $M^{*G}(t)$ is the state of efferent firing with highest statistical weight. Therefore, it is natural to explore mechanisms which favor common highly weighted efferent and afferent firings in ranges consistent with favorable firing threshold factors $F^G \approx 0$.

A model of dominant inhibition describes how minicolumnar firings are suppressed by their neighboring minicolumns. For example, this could be effected by developing NN mesocolumnar interactions (Ingber, 1983), but here the averaged effect is established by inhibitory mesocolumns (Case I) by setting $A_E^I = A_I^E = 2A_E^E = 0.01N^*/N$. Since there appears to be relatively little $I - I$ connectivity, set $A_I^I = 0.0001N^*/N$. The background synaptic noise is taken to be $B_I^E = B_E^I = 2B_E^E = 10B_I^I = 0.002N^*/N$. As minicolumns are observed to have ~110 neurons (visual cortex appears to have approximately twice this density) (Mountcastle, 1978), and as there appear to be a predominance of E over I neurons (Nunez, 1981), here take $N^E = 80$ and $N^I = 30$. Use $N^*/N = 10^3$, $v_{G'}^G$, and $\phi_{G'}^G$ as estimated previously. The "threshold factors" F_I^G for this I model are then

$$F_I^E = \frac{(0.5\bar{M}^I - 0.25\bar{M}^E + 3.0)}{\pi^{1/2}(0.1\bar{M}^I + 0.05\bar{M}^E + 9.80)^{1/2}} \ ,$$

$$F_I^I = \frac{(0.005\bar{M}^I - 0.5\bar{M}^E - 45.8)}{\pi^{1/2}(0.001\bar{M}^I + 0.1\bar{M}^E + 11.2)^{1/2}} \ . \tag{4}$$

In the prepoint-discretized deterministic limit, the threshold factors determine when and how smoothly the step-function forms $\tanh F_I^G$ in $g^G(t)$ change $M^G(t)$ to $M^G(t + \tau)$. F_I^I will cause afferent $\bar{M}^I$ to fire for most of its values, as $\bar{M}^I \sim -N^I \tanh F_I^I$ will be positive for most values of $\bar{M}^G$ in F_I^I, which is already

weighted heavily with a term -45.8. Looking at F_I^E, it is seen that the relatively high positive values of efferent $\bar{M}^I$ require at least moderate values of positive efferent $\bar{M}^E$ to cause firings of afferent $\bar{M}^E$.

The centering effect of the I model, labeled here as the IC model, is quite easy for neocortex to accommodate. For example, this can be accomplished simply by readjusting the synaptic background noise from B_E^G to B'^G_E,

$$B'^G_E = \frac{[V^G - (\frac{1}{2} A_I^G + B_I^G)v_I^G N^I - \frac{1}{2} A_E^G v_E^G N^E]}{v_E^G N^G} \tag{5}$$

for both $G = E$ and $G = I$. In general, B_E^G and B_I^G (and possibly A_E^G and A_I^G due to actions of neuromodulators, and J_G constraints from long-ranged fibers) are available to zero the constant in the numerator, giving an extra degree(s) of freedom to this mechanism. (If B'^G_E would be negative, this leads to unphysical results in the square-root denominator of F^G. Here, in all examples where this occurs, it is possible to instead find positive B'^G_I to appropriately shift the numerator of F^G.) In this context, it is empirically observed that the synaptic sensitivity of neurons engaged in selective attention is altered, presumably by the influence of chemical neuromodulators on postsynaptic neurons (Mountcastle, Andersen & Motter, 1981).

By this Centering mechanism, $B'^E_E = 1.38$ and $B'^I_I = 15.3$, and F_I^G is transformed to F_{IC}^G,

$$F_{IC}^E = \frac{(0.5\bar{M}^I - 0.25\bar{M}^E)}{\pi^{1/2}(0.1\bar{M}^I + 0.05\bar{M}^E + 10.4)^{1/2}} ,$$

$$F_{IC}^I = \frac{(0.005\bar{M}^I - 0.5\bar{M}^E)}{\pi^{1/2}(0.001\bar{M}^I + 0.1\bar{M}^E + 20.4)^{1/2}} . \tag{6}$$

Note that, aside from the enforced vanishing of the constant terms in the numerators of F_I^G, the only other changes in F_I^G moderately affect the constant terms in the denominators.

The other "extreme" of normal neocortical firings is a model of dominant excitation, effected by establishing excitatory mesocolumns (Case E) by using the same parameters $\{B_{G'}^G, v_{G'}^G, \phi_{G'}^G, A_I^I\}$ as in the I model, but setting $A_E^E = 2A_E^I = 2A_I^E = 0.01N^*/N$. This yields

$$F_E^E = \frac{(0.25\bar{M}^I - 0.5\bar{M}^E - 24.5)}{\pi^{1/2}(0.05\bar{M}^I + 0.10\bar{M}^E + 12.3)^{1/2}} ,$$

$$F_E^I = \frac{(0.005\bar{M}^I - 0.25\bar{M}^E - 25.8)}{\pi^{1/2}(0.001\bar{M}^I + 0.05\bar{M}^E + 7.24)^{1/2}} . \tag{7}$$

The negative constant in the numerator of F_E^I inhibits afferent $\bar{M}^I$ firings. Although there is also a negative constant in the numerator of F_E^E, the increased coefficient of $\bar{M}^E$ (relative to its corresponding value in F_I^E), and the fact that $\bar{M}^E$ can range up to $N^E = 80$, readily permits excitatory firings throughout most of the range of $\bar{M}^E$.

Applying the Centering mechanism to E, $B'^E_I = 10.2$ and $B'^I_I = 8.62$. The net effect in F_{EC}^G, in addition to removing the constant terms in the numerators of F_E^G, is to change the constant terms in the denominators: 12.3 in F_E^E is changed to 17.2 in F_{EC}^E, and 7.24 in F_E^I is changed to 12.4 in F_{EC}^I.

Now it is natural to examine a balanced Case intermediate between I and E, labeled here as Case B. This is accomplished by changing $A_E^E = A_E^I = A_I^E = 0.005N^*/N$. This yields

$$F_B^E = \frac{(0.25\bar{M}^I - 0.25\bar{M}^E - 4.50)}{\pi^{1/2}(0.050\bar{M}^E + 0.050\bar{M}^I + 8.30)^{1/2}} ,$$

$$F_B^I = \frac{(0.005\bar{M}^I - 0.25\bar{M}^E - 25.8)}{\pi^{1/2}(0.001\bar{M}^I + 0.050\bar{M}^E + 7.24)^{1/2}} . \tag{8}$$

Applying the Centering mechanism to B, $B'^E_E = 0.438$ and $B'^I_I = 8.62$. The net effect in F^G_{BC}, in addition to removing the constant terms in the numerators of F^G_B, is to change the constant terms in the denominators: 8.30 in F^E_B is changed to 7.40 in F^E_{BC}, and 7.24 in F^I_B is changed to 12.4 in F^I_{BC}.

2.6.4. Inclusion of Macroscopic Circuitry

The most important features of this development are described by the Lagrangian $\underline{L}^G$ in the negative of the argument of the exponential describing the probability distribution, and the "threshold factor" F^G describing an important sensitivity of the distribution to changes in its variables and parameters.

To more properly include long-ranged fibers, when it is possible to numerically include interactions among macrocolumns, the J_G terms can be dropped, and more realistically replaced by a modified threshold factor F^G,

$$F^G = \frac{(V^G - a^{|G|}_{G'} v^{|G|}_{G'} N^{G'} - \frac{1}{2} A^{|G|}_{G'} v^{|G|}_{G'} M^{G'} - a^{\ddagger E}_{E'} v^E_{E'} N^{\ddagger E'} - \frac{1}{2} A^{\ddagger E}_{E'} v^E_{E'} M^{\ddagger E'})}{((\pi/2)[(v^{|G|}_{G'})^2 + (\phi^{|G|}_{G'})^2](a^{|G|}_{G'} N^{G'} + \frac{1}{2} A^{|G|}_{G'} M^{G'} + a^{\ddagger E}_{E'} N^{\ddagger E'} + \frac{1}{2} A^{\ddagger E}_{E'} M^{\ddagger E'}))^{1/2}} \; ,$$

(9)

$$a^{\ddagger E}_{E'} = \frac{1}{2} A^{\ddagger E}_{E'} + B^{\ddagger E}_{E'} \; .$$

Here, afferent contributions from $N^{\ddagger E}$ long-ranged excitatory fibers, e.g., cortico-cortical neurons, have been added, where $N^{\ddagger E}$ might be on the order of 10% of N^*: Of the approximately 10^{10} to 10^{11} neocortical neurons, estimates of the number of pyramidal cells range from 1/10 to 2/3. Nearly every pyramidal cell has an axon branch that makes a cortico-cortical connection; i.e., the number of cortico-cortical fibers is of the order 10^{10}.

The long-ranged circuitry was parameterized (with respect to strengths and time delays) in the EEG studies described above. In this way SMNI presents a powerful computational tool to include both long-ranged global regional activity and short-ranged local columnar activity.

2.7. Portfolio of Physiological Indicators (PPI)

The SMNI distributions present a template for distributions of neocortical populations. The Trading in Risk Dimensions (TRD) project illustrates how such distributions can be developed as a Portfolio of Physiological Indicators (PPI) (Ingber, 2005), to calculate risk and uncertainty of functions, e.g., functions of Ideas, dependent on events that impact populations of neurons (Ingber, 2006b).

It is clear that the SMNI distributions also can be used to process different imaging data beyond EEG, e.g., also MEG, PET, SPECT, fMRI, etc., where each set of imaging data is used to fit it own set of parameterized SMNI distributions using a common regional circuitry. (Different imaging techniques may have different sensitivities to different synaptic and neuronal activities.) Then, portfolios of these imaging distributions can be developed to describe the total neuronal system, e.g., akin to a portfolio of a basket of markets. For example, this could permit the uncertainties of measurements to be reduced by weighting the contributions of different data sets, etc. Overlaps of distributions corresponding to different subsets of data give numerical specificity to the values of using these subsets.

It is to be expected that better resolution of behavioral events can be determined by joint distributions of different imaging data, rather than by treating each distribution separately.

2.7.1. Local Versus Global Influences

Another twist on the use of this approach is to better understand the role of local and global contributions to imaging data. EEG data is often collected at different electrode resolutions. Cost functions composed of these different collection-method variables can be used to calculate expectations over their imaging portfolios. For example, relative weights of two scales of collection methods can be fit as parameters, and relative strengths as they contribute to various circuitries can be calculated. This method will be applied

to determine the degree of relevance of local and global activity during specific tasks. If some tasks involve circuitry with frontal cortex, then these methods may contribute to the understanding of the role of consciousness.

2.8. Application to Ideas by Statistical Mechanics (ISM)

These kinds of applications of SMNI and TRD to PPI have obvious counterparts in an AI approach to Ideas by Statistical Mechanics (ISM). ISM is a generic program to model evolution and propagation of ideas/patterns throughout populations subjected to endogenous and exogenous interactions. The program is based on the author's work in SMNI, and uses the author's ASA code (Ingber, 1993a) for optimizations of training sets, as well as for importance-sampling to apply the author's copula financial risk-management codes, TRD (Ingber, 2005), for assessments of risk and uncertainty. This product can be used for decision support for projects ranging from diplomatic, information, military, and economic (DIME) factors of propagation/evolution of ideas, to commercial sales, trading indicators across sectors of financial markets, advertising and political campaigns, etc. It seems appropriate to base an approach for propagation of ideas on the only system so far demonstrated to develop and nurture ideas, i.e., the neocortical brain (Ingber, 2006a; Ingber, 2007; Ingber, 2008).

3. Euler-Lagrange (EL) Equations

To investigate dynamics of multivariate stochastic nonlinear systems, such as neocortex presents, it is not sensible to simply apply simple mean-field theories which assume sharply peaked distributions, since the dynamics of nonlinear diffusions in particular are typically washed out. Here, path integral representations of systems, otherwise equivalently represented by Langevin or Fokker-Planck equations, present elegant algorithms by use of variational principles leading to Euler-Lagrange equations (Langouche, Roekaerts & Tirapegui, 1982).

The Euler-Lagrange equations are derived from the variational principle possessed by the SMNI Lagrangian L, essentially the counterpart to force equals mass times acceleration,

$$\frac{\partial}{\partial t}\frac{\partial L}{\partial(\partial\Phi/\partial t)} + \frac{\partial}{\partial x}\frac{\partial L}{\partial(\partial\Phi/\partial x)} - \frac{\partial L}{\partial\Phi} = 0 \ . \tag{10}$$

where x represent the independent dynamical variable. Below there are two variables $\{M^E, M^I\}$ considered with two coupled equations. The result is

$$\alpha\frac{\partial^2\Phi}{\partial t^2} + \beta\frac{\partial^2\Phi}{\partial x^2} + \gamma\Phi - \frac{\partial F}{\partial\Phi} = 0 \ . \tag{11}$$

because the determinant prefactor g defined above also contains nonlinear details affecting the state of the system. Since g is often a small number, distortion of the scale of L is avoided by normalizing g/g_0, where g_0 is simply g evaluated at $M^E = M^{\ddagger E'} = M^I = 0$. Φ was developed in earlier papers to be the measured scalp electric potential, a function of the underlying columnar firings (Ingber & Nunez, 1990).

If there exist regions in neocortical parameter space such that we can identify $\beta/\alpha = -c^2$, $\gamma/\alpha = \omega_0^2$ (e.g., as explicitly calculated using the centering mechanism),

$$\frac{1}{\alpha}\frac{\partial F}{\partial\Phi} = -\Phi f(\Phi) \ , \tag{12}$$

and we take x to be one-dimensional in the narrow parabolic trough described above, then we recover the nonlinear string model mentioned in the Introduction.

The most-probable firing states derived variationally from the path-integral Lagrangian as the Euler-Lagrange equations represent a reasonable average over the noise in the SMNI system, which can be equivalently written as a Langevin system of coupled stochastic differential equations, a multivariate Fokker-Planck partial differential equation, or as a path-integral over a conditional probability distribution (Ingber, 1982; Ingber, 1983).

For many studies, the noise cannot be simply disregarded, as demonstrated in other SMNI STM and EEG studies, but for the purpose here of demonstrating the existence of multiple local oscillatory states that can be identified with EEG frequencies, the EL equations serve very well.

Note that there can be a dozen spatial-temporal coupled EL equations for SMNI systems even for local studies, as derived in previous SMNI papers (Ingber, 1983; Ingber, 1995a).

Previous SMNI EEG studies have demonstrated that simple dispersion relations derived from the EL equations support the local generation of alpha frequencies as observed experimentally as well as deriving diffusive propagation velocities of information across minicolumns consistent with other experimental studies.. The earliest studies simply used a driving force $J_G M^G$ in the Lagrangian to model long-ranged interactions among fibers (Ingber, 1982; Ingber, 1983). Subsequent studies considered regional interactions driving localized columnar activity within these regions (Ingber, 1996b; Ingber, 1997; Ingber, 1998). This study considers self-sustaining EEG activity within columns.

In this study, we consider a fully coupled local system of $E - I$ firing states, without any other *ad hoc* driving forces.

$$c_{12}^{E\ddot{E}} \ddot{M}^E + c_{13}^{E\dot{E}} \dot{M}^E + c_{21}^{E\dot{E}^2} (\dot{M}^E)^2 + c_{22}^{E\dot{I}} \dot{M}^I + c_{23}^{E\dot{I}^2} (\dot{M}^I)^2 + c_{11}^{E\bar{E}} M^E + c_{51}^{E} \, 1 = 0$$

$$c_{32}^{I\ddot{E}} \ddot{M}^I + c_{33}^{I\dot{E}} \dot{M}^E + c_{41}^{I\dot{E}^2} (\dot{M}^E)^2 + c_{42}^{I\dot{I}} \dot{M}^I + c_{43}^{I\dot{I}^2} (\dot{M}^I)^2 + c_{31}^{I\bar{E}} M^I + c_{52}^{I} \, 1 = 0 \qquad (13)$$

This set of coupled EL equations is in terms of 14 coefficients, each of which is a function of the two firing states, $c = c(M^E, M^I)$. The double-digit subscripts $\{c_{ij}\}$ are used to identify row-column graphs in figures below.

That is, the highly nonlinear EL equations have been greatly simplified by imagining that at each point in the numerical mesh describing the firing space $\{M^E, M^I\}$ a Taylor expansion of each term in the EL equations is performed, keeping coefficients up to order $\{M^G, \dot{M}^G, (\dot{M}^G)^2\}$ with a residual term constant at this point in this firing space. It is noted that some areas of coarser mesh exhibit similar structures, and this is the basis of looking further for oscillatory behavior within these ranges of columnar firings.

3.1. Maxima, Gnuplot and C codes

Maxima output can be directly converted to Fortran, and then the f2c utility can be used to generate C code. However, that C code is barely readable and thus hard to maintain. Instead, Maxima output can be directly processed a few simple Unix scripts to generate very decent standard C code. If the columnar parameters are left unspecified, then some of the EL coefficients can be as long as several hundred thousand lines, but which compile well under gcc/g++. This code can be useful for future fits of these parameters to actual clinical data, similar to the EEG project discussed above.

A great advantage of using an algebraic language like Maxima over numerical languages like C/C++ is that highly nonlinear expressions can be processed before numerical specifications, often keep small but important scales without losing them to round-off constraints.

The numerical output of Maxima is then developed by Gnuplot (Williams & Kelley, 2008) into graphs presented here.

3.2. Results

Calculations of coefficients of EL equations were performed for three prototypical firing case established in earlier SMNI papers (Ingber, 1984), predominately excitatory (E), predominately inhibitory (I) and balanced about evenly (B). More minima can be brought within physical firing ranges when a "Centering" mechanism is invoked (Ingber, 1984), by tuning the presynaptic stochastic background, a phenomena observed during selective attention, giving rise to cases EC, IC and BC. The states BC are observed to yield properties of auditory STM, e.g., the 7 ± 2 capacity rule and times of duration of these memory states (Ingber, 1984; Ingber, 1985c).

It is observed that visual neocortex has twice the number of neurons per minicolumn as other regions of neocortex. In the SMNI model this gives rise to fewer and deeper STM states, consistent with the observed 4 ± 2 capacity rule of these memory states. These calculations are cases ECV, ICV and BCV.

Calculations here took into account that regions of small M^G have more detailed structure for the most interesting Centered cases, by stepping the mesh according to

$$\Delta M^G = floor((abs(M^G)/10 + 1)) . \qquad (14)$$

This discrete mesh develops M^G space into 1908 point for non-visual cortex and 3216 points for visual cortex. All graphs presented here invoked some thresholds to present structures within physical ranges of experimentally observed phenomena. All absolute values lying outside of these thresholds are not plotted (although they are retained in data files). Plots of the EL coefficients used thresholds of 0.5. Plots of the Lagrangian used thresholds of 0.5. (Earlier SMNI studies set Lagrangian thresholds at 0.04.) Cases E, EC and ECV are given in Figures 3-5. Cases I, IC and ICV are given in Figures 6-8. Cases B, BC and BCV are given in Figures 9-11.

It is interesting to note some relationships between the "mass x acceleration" term of the EL equations, essentially the diffusion times the second derivatives of M^G, with the string-"force" term proportional to M^G to motivate looking for oscillatory states. However, only complete calculations involving all terms can deliver the results given below.
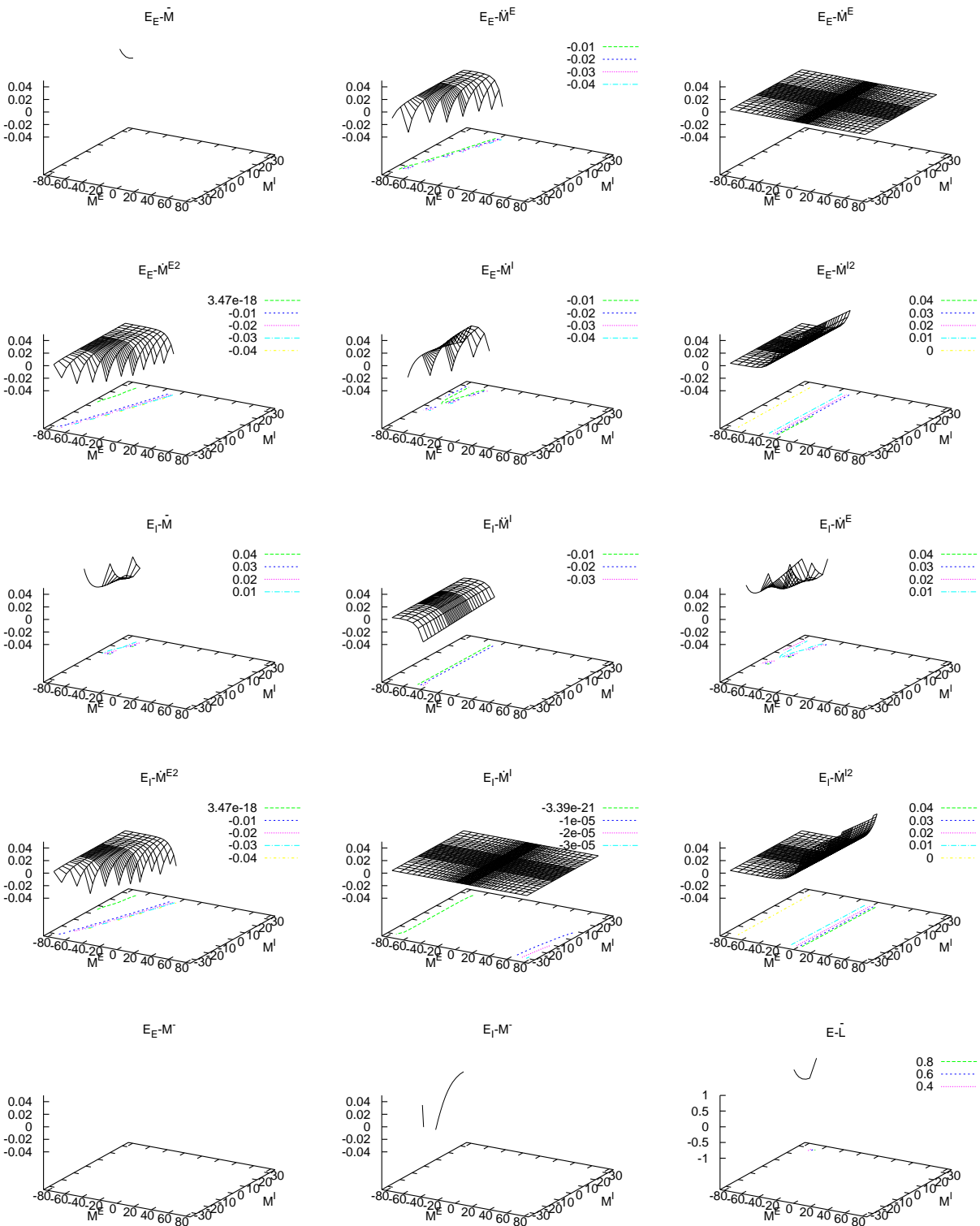
Fig. 3. Euler-Lagrange coefficients for Excitatory neocortical columnar firings. See Eq. (13) for identification of graphs with EL coefficients $\{c_{ij}\}$. Bottom right corner graph (location 53) is the Lagrangian.
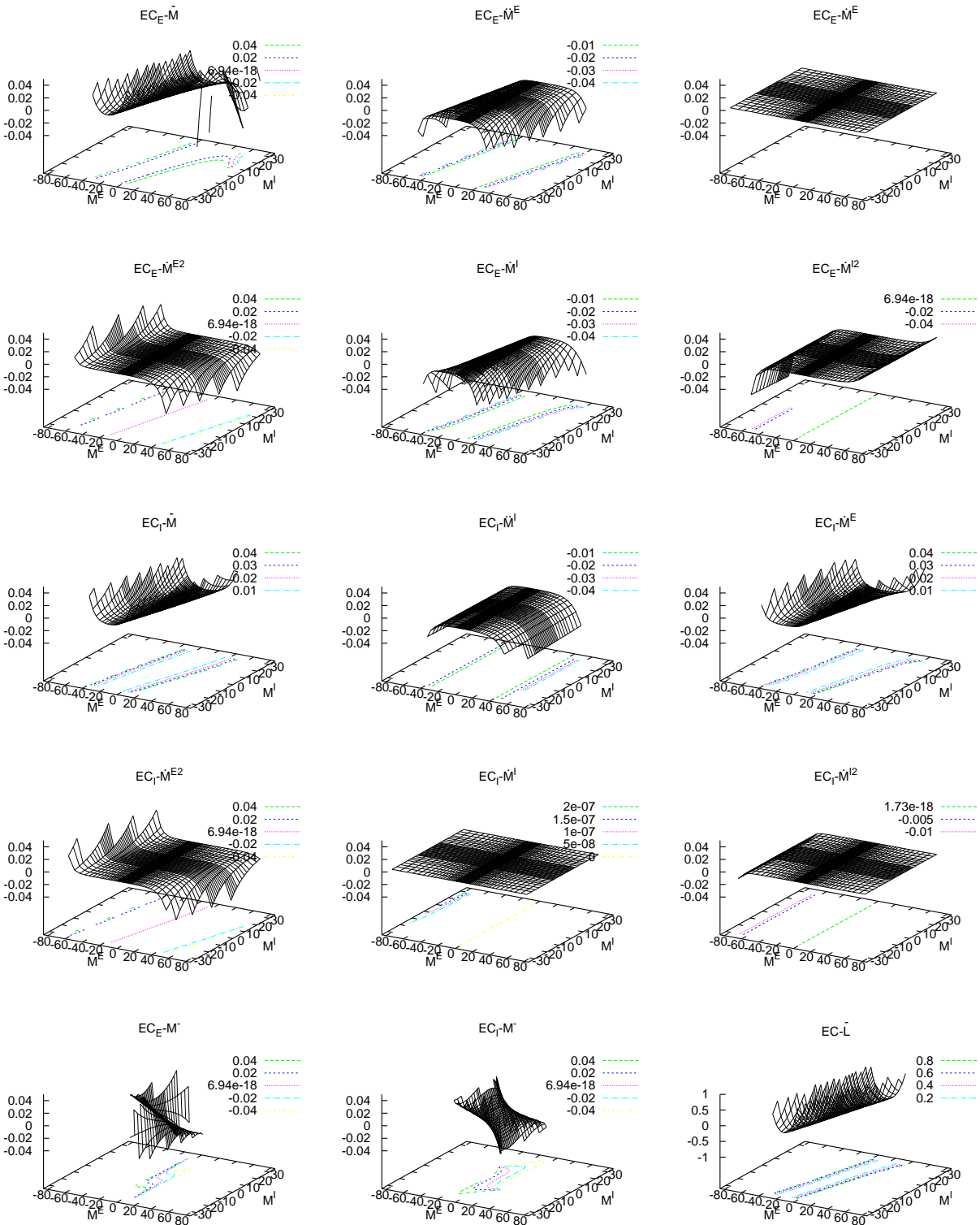
Fig. 4. Euler-Lagrange coefficients for Excitatory Centered neocortical columnar firings. See Eq. (13) for identification of graphs with EL coefficients $\{c_{ij}\}$. Bottom right corner graph (location 53) is the Lagrangian.
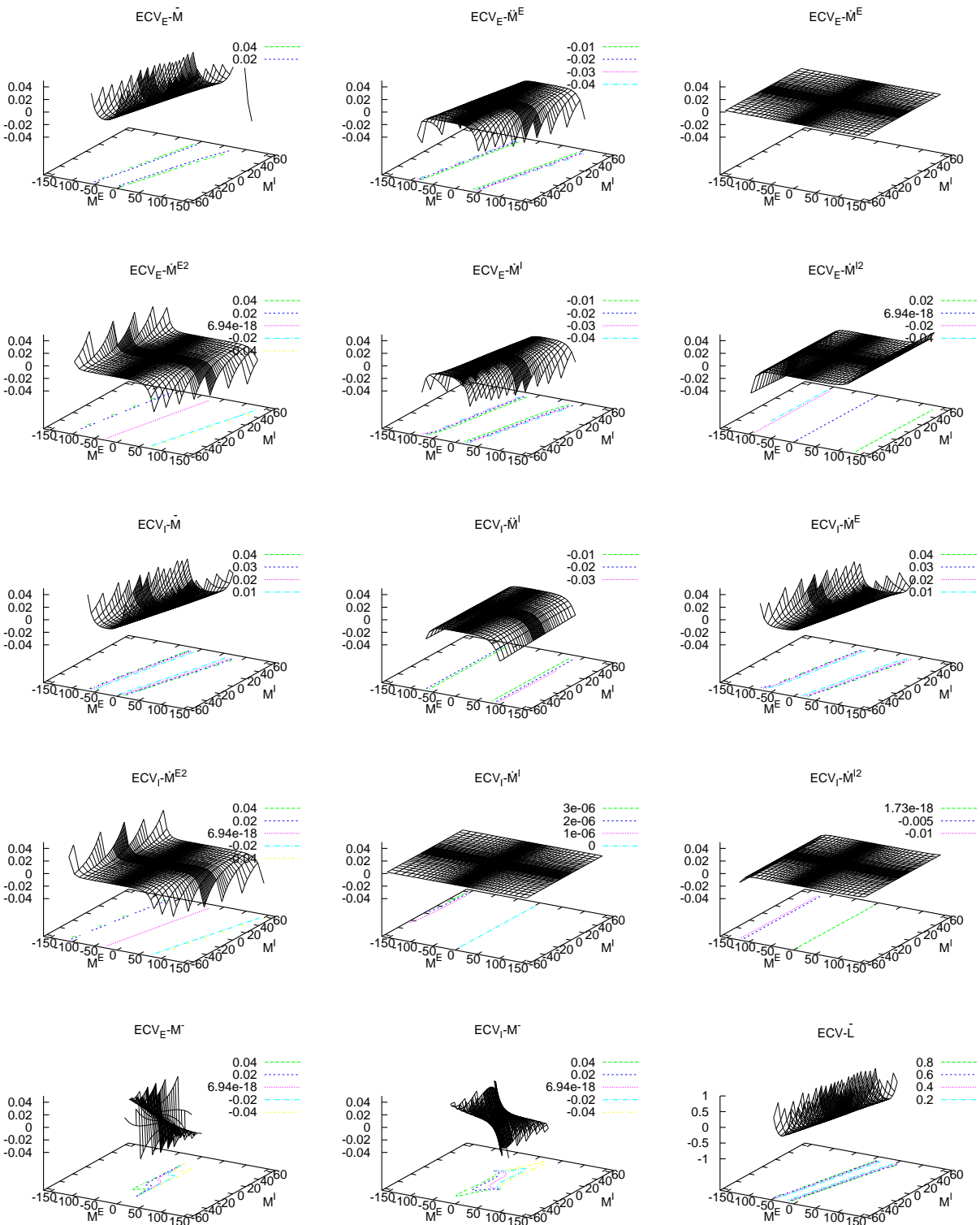
Fig. 5. Euler-Lagrange coefficients for Excitatory Centered Visual neocortical columnar firings. See Eq. (13) for identification of graphs with EL coefficients $\{c_{ij}\}$. Bottom right corner graph (location 53) is the Lagrangian.
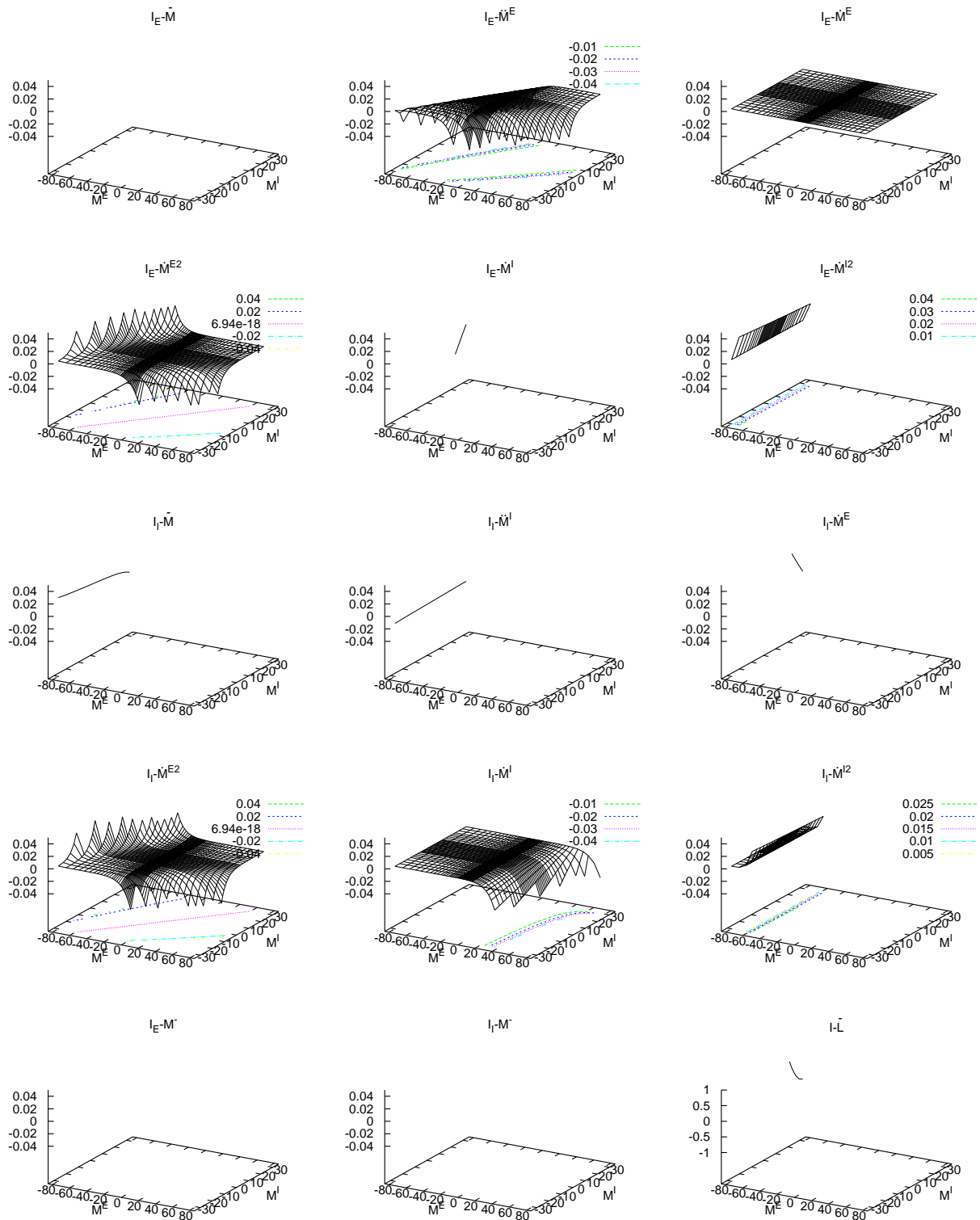
Fig. 6. Euler-Lagrange coefficients for Inhibitory neocortical columnar firings. See Eq. (13) for identification of graphs with EL coefficients $\{c_{ij}\}$. Bottom right corner graph (location 53) is the Lagrangian.
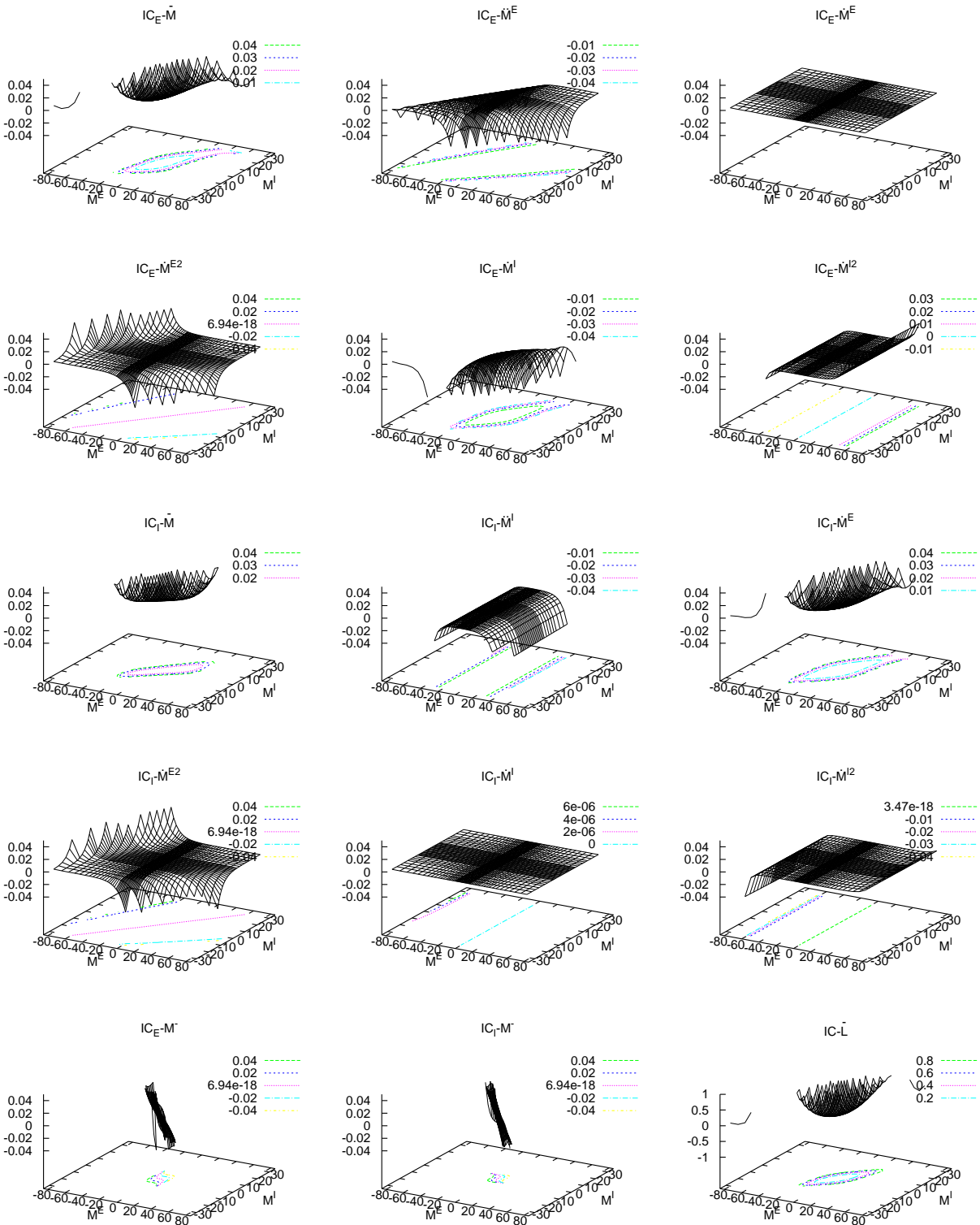
Fig. 7. Euler-Lagrange coefficients for Inhibitory neocortical columnar firings. See Eq. (13) for identification of graphs with EL coefficients $\{c_{ij}\}$. Bottom right corner graph (location 53) is the Lagrangian.
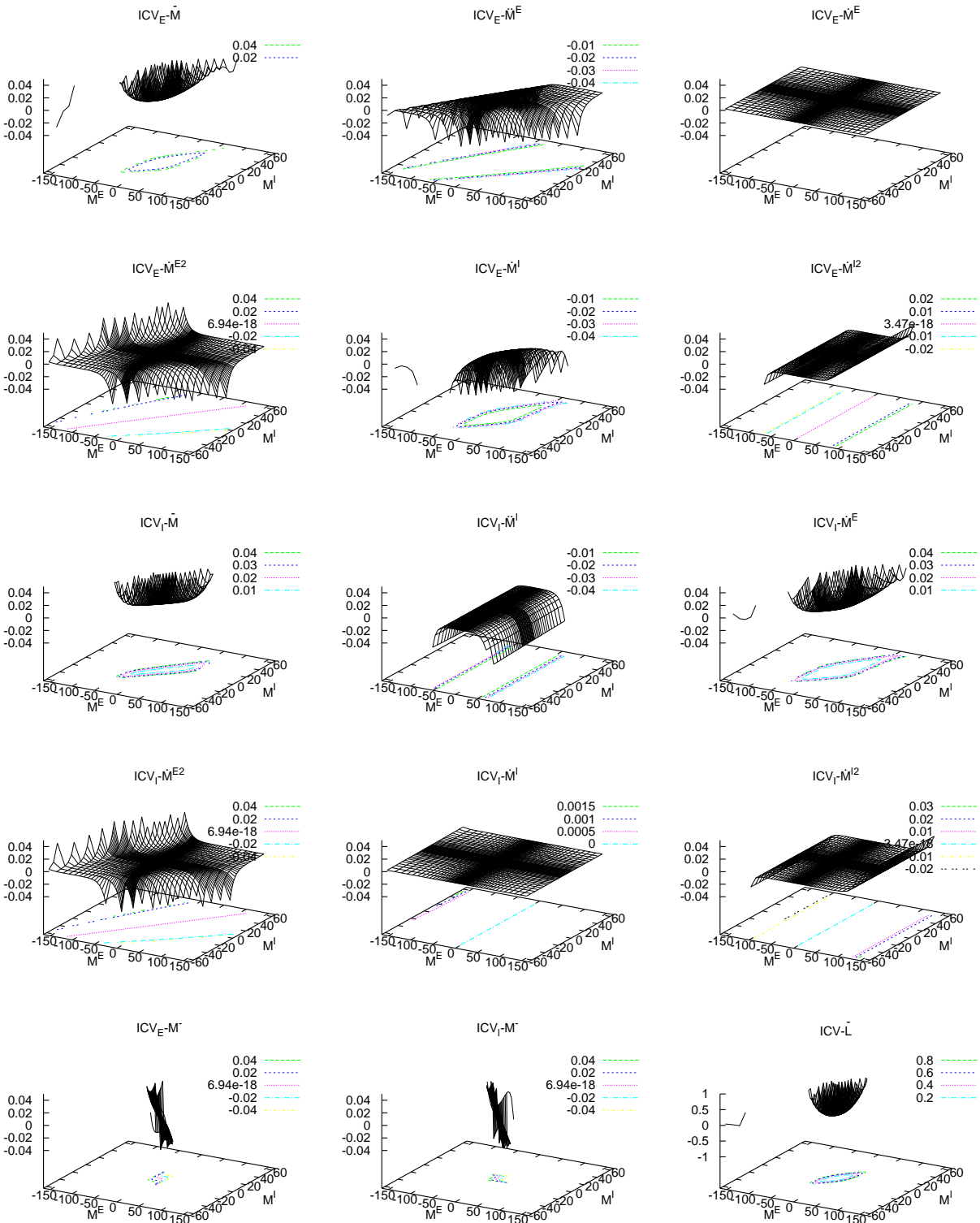
Fig. 8. Euler-Lagrange coefficients for Inhibitory neocortical columnar firings. See Eq. (13) for identification of graphs with EL coefficients $\{c_{ij}\}$. Bottom right corner graph (location 53) is the Lagrangian.
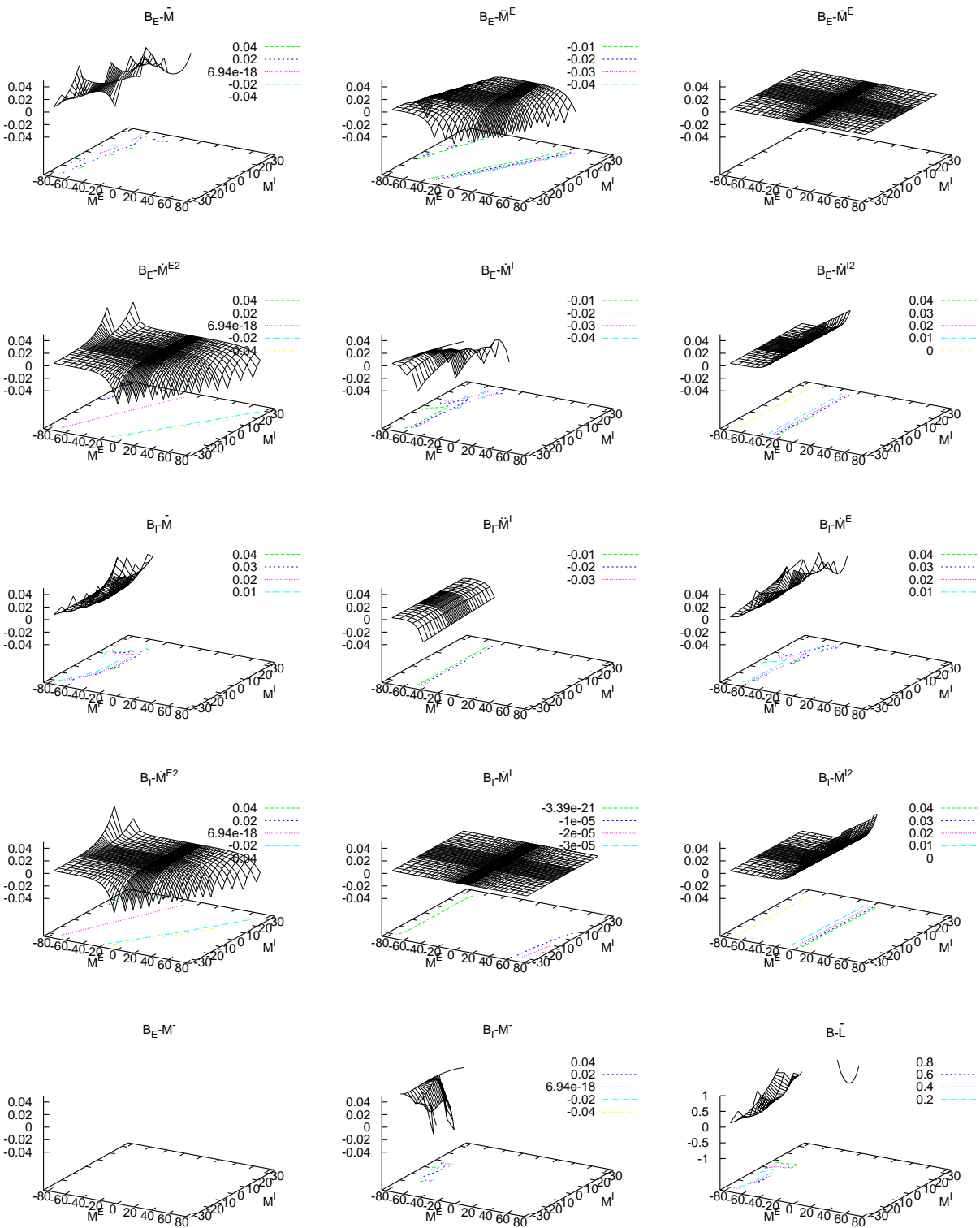
Fig. 9. Euler-Lagrange coefficients for Balanced neocortical columnar firings. See Eq. (13) for identification of graphs with EL coefficients $\{c_{ij}\}$. Bottom right corner graph (location 53) is the Lagrangian.
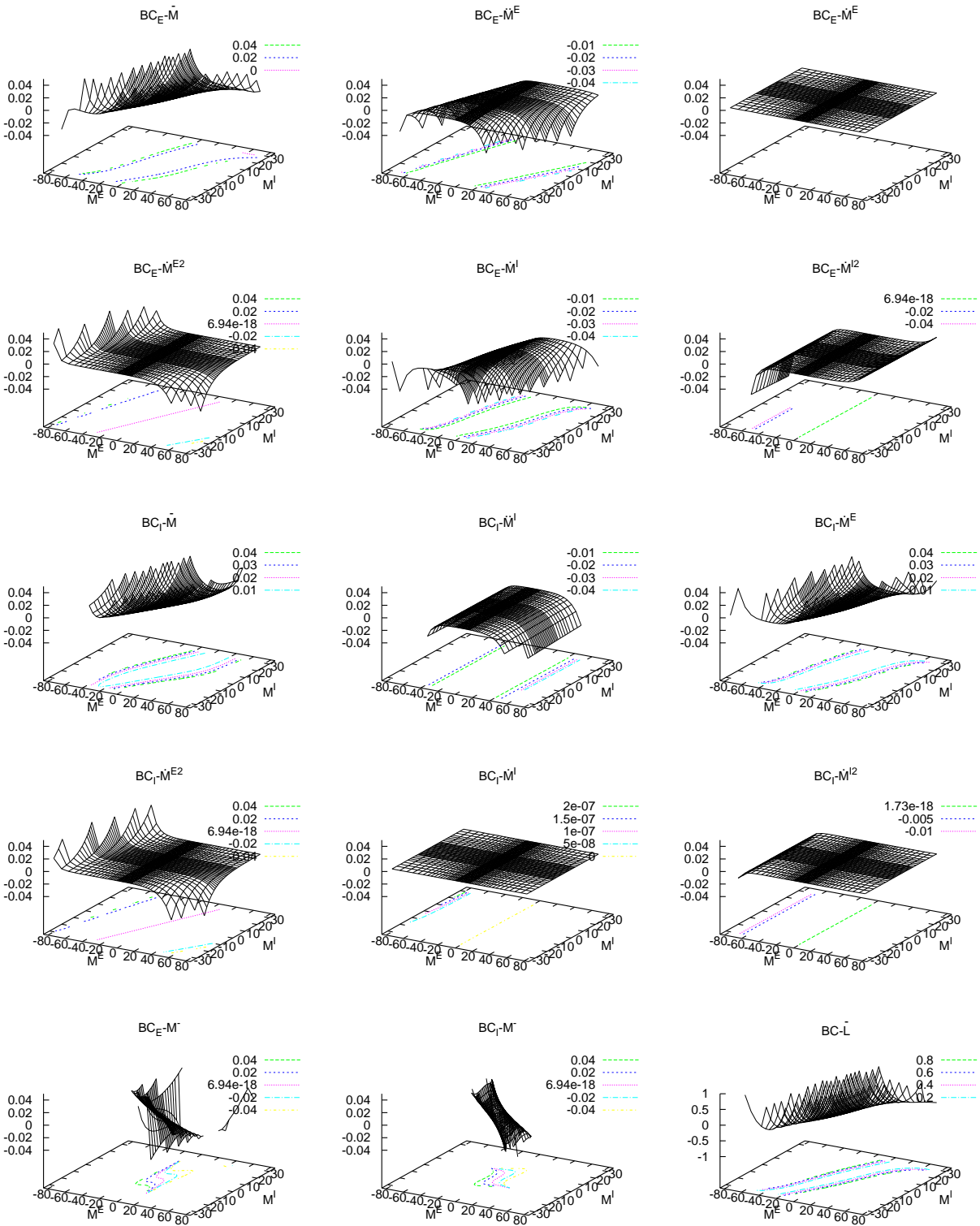
Fig. 10. Euler-Lagrange coefficients for Balanced neocortical columnar firings. See Eq. (13) for identification of graphs with EL coefficients $\{c_{ij}\}$. Bottom right corner graph (location 53) is the Lagrangian.
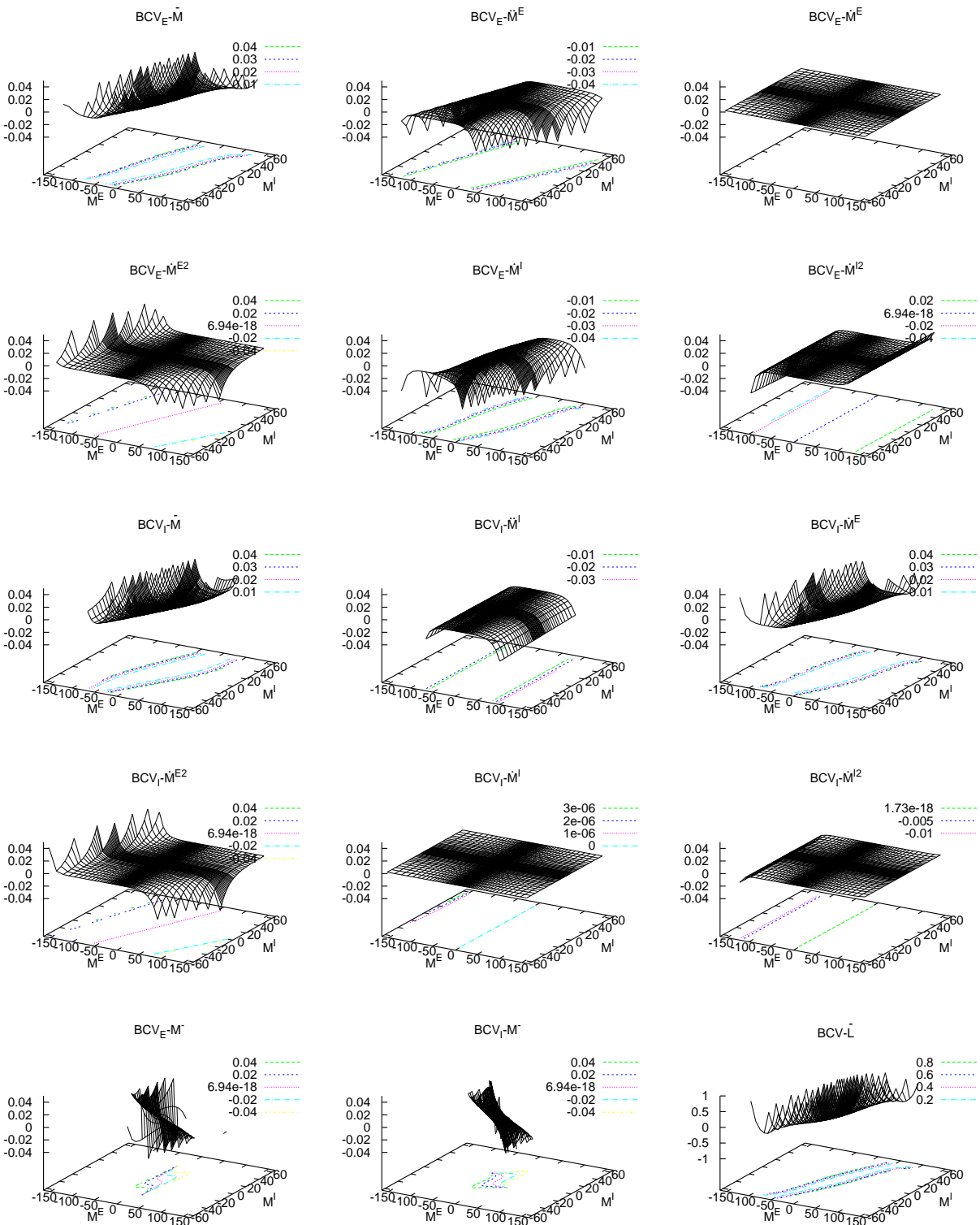
Fig. 11. Euler-Lagrange coefficients for Balanced neocortical columnar firings. See Eq. (13) for identification of graphs with EL coefficients *{c_{ij}}*. Bottom right corner graph (location 53) is the Lagrangian.

4. Correction of sqrt(2) Error

A $\sqrt{2}$ error has been propagated in a series of papers spanning 1981-2008. As first published in 1982 (Ingber, 1982), in the calculation of

$$p_{\sigma_j} = \pi^{-\frac{1}{2}} \int\limits_{(\sigma_j F_j \sqrt{\pi}/2)}^{\infty} dz \; exp(-z^2) = \frac{1}{2}[1 - \mathrm{erf}(\sigma_j F_j \sqrt{\pi}/2)], \tag{15}$$

$$F_j = (V_j - \sum_k a_{jk} v_{jk})/[\pi \sum_{k'} a_{jk'}(v_{jk'}^2 + \phi_{jk'}^2)]^{\frac{1}{2}} . \tag{16}$$

the last equation, F_j should be corrected with a $\sqrt{2}$, as in

$$F_j = (V_j - \sum_k a_{jk} v_{jk})/[(\pi/2) \sum_{k'} a_{jk'}(v_{jk'}^2 + \phi_{jk'}^2)]^{\frac{1}{2}} . \tag{17}$$

This also similarly affects all mesocolumnar averages over neuronal F_j, yielding F^G factors in subsequent algebra.

In this paper, calculations of the Balanced centered case with this $\sqrt{(2)}$ error is case BC2, to be compared with calculations of case BC. This error has no dramatic consequences on other results derived in the above papers. This is because in all these papers, regarding $(v_{jk'}^2 + \phi_{jk'}^2)$, only numerical values of 0.1^2 values have been used for $v_{jk'}^2$ and $\phi_{jk'}^2$. Thus, this would only have the numerical effect of increasing ϕ by a factor of 1.73 (a number not well established experimentally): $0.1^2 + 0.1^2 = 0.02 \rightarrow 2(0.02) = 0.04 = 0.1^2 + \sqrt{0.03}^2 = 0.1^2 + 0.173^2$, where $qv_{jk'}$ is the mean and $q\phi_{jk'}^2$ is the variance of Γ, in mV, of the postsynaptic response to q quanta. Therefore, this also presents an opportunity to see how robust the SMNI model is with respect to changes in synaptic parameters within their experimentally observed ranges.

The nature of the modifications is illustrated in Figure 12, to be compared with results using the correct equations in Figure 10. While care has been taken to use only neocortical parameters with values within experimental observations, these values can range substantially, and so any results such as those presented here could be just as reasonable if interpolated or reasonably extrapolated between these two figures.
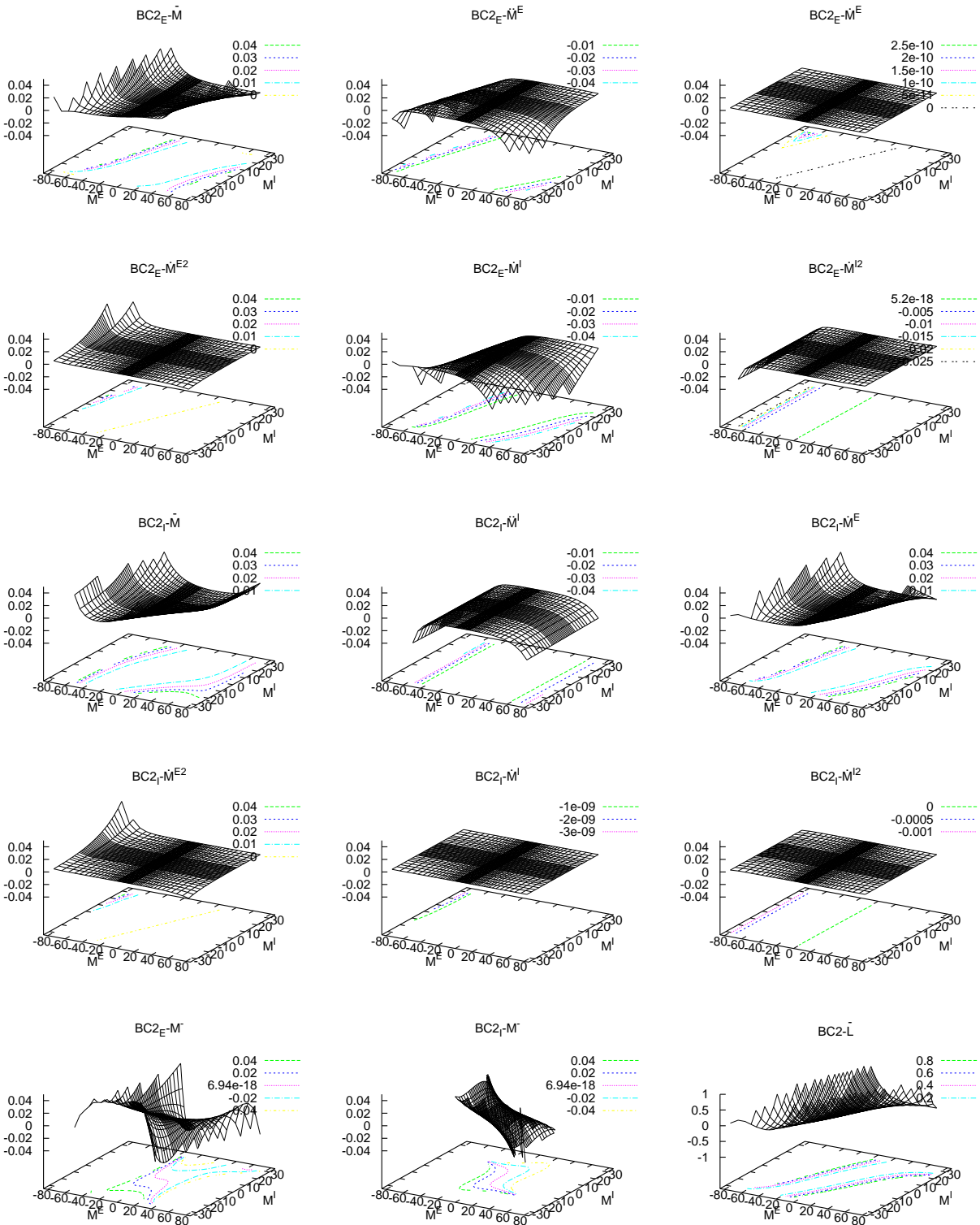
Fig. 12. Euler-Lagrange coefficients for Balanced neocortical columnar firings with original $\sqrt{2}$ error. See Eq. (13) for identification of graphs with EL coefficients $\{c_{ij}\}$. Bottom right corner graph (location 53) is the Lagrangian.

5. Oscillatory States Supported by SMNI EL Equations

After the Taylor expansions are taken, each of the EL terms in the neighborhood of the M-dependent terms is assumed to have a dependence,

$$M^G \rightarrow M^G \exp(-i\omega_G t) \tag{18}$$

where ω_G (independent ω_E and ω_I) can be complex, and for brevity the same notation M^G is used in the ω_G-transformed space. The real part of ω_G represents oscillatory states, while the imaginary part represent attenuation in time of these states. If in fact there are some finite neighborhoods in M^G space that supports real ω, with only modest attenuation, then it can be claimed that these neighborhoods support oscillatory states. The motivation of this study was to seek such states within experimentally observed ranges and to see if there could be multiple frequencies spanning observed theta, alpha and beta frequencies.

Note that if the time scales of postsynaptic response, τ, is on the order of 10 msec, then $\omega_G \tau$ (which is what is being calculated) on the order of 1 is equivalent to a frequency $\nu_G = \omega_G/(2\pi)$ on the order of 16 cps (Hz) which is close to the range of observed alpha rhythms (considered to be 8-12 Hz).

At each point in M^G space a simple generalization of Newton's method, mnewton within Maxima set to a limit of 50 iterations per point in firing space, was used to try to solve the couple EL equations for complex ω_G. In some instances no reasonable neighborhoods for real ω_G could be found. The code mnewton is called 109,150 times (with 50 iterations per each call) for the calculations presented here, and this routine was clearly picked solely for its speed. All graphs presented here invoked some thresholds to present structures within physical ranges of experimentally observed phenomena. All absolute values lying outside of these thresholds are not plotted (although they are retained in data files). Plots of the frequencies used thresholds of 10.0. (The can be many roots at higher and lower values due to combinations of polynomials and sinusoidal functions in ω_G.) As can be seen in the graphs in Figures 13-17, there are many regions supporting $\omega_G \tau$ ranging from 0.1 to 10.

In clinical settings is observed that frequencies understood as alpha often in fact show components of varying frequencies especially around 8-13 Hz. When even higher resolutions of EEG are obtained, e.g., below the scalp, multiple components are more obvious, and even local patches of EEG may be observed (Nunez & Srinivasan, 2006; Nunez, 2009).
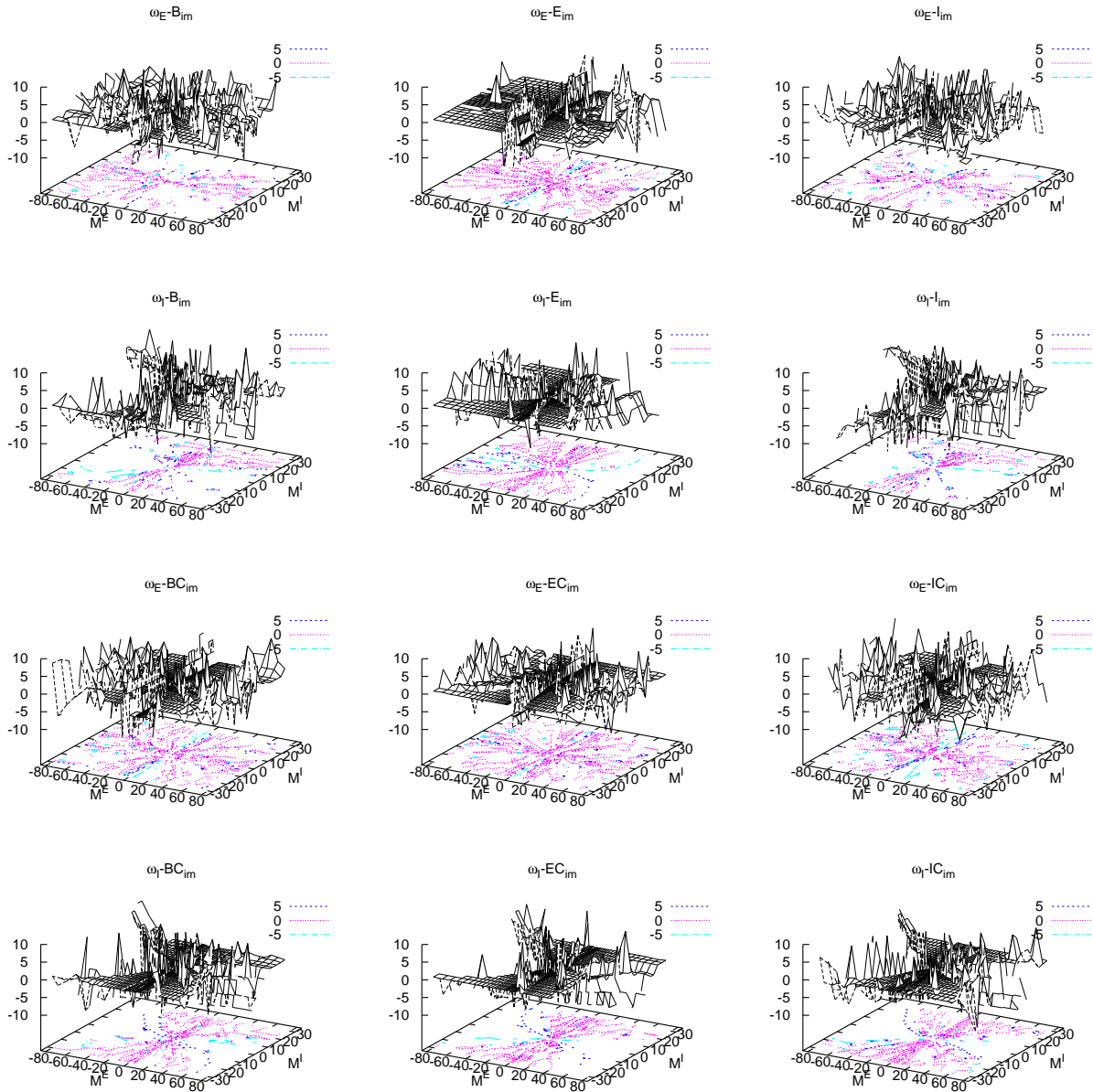
Fig. 13. Real (oscillatory) frequency solutions for Balanced, Excitatory and Inhibitory neocortical columnar firings, in columns 1-3 resp. Rows 3 and 4 are these cases with the centering mechanism. Solutions in rows 1 and 3 are ω_E, rows 2 and 4 are ω_I.
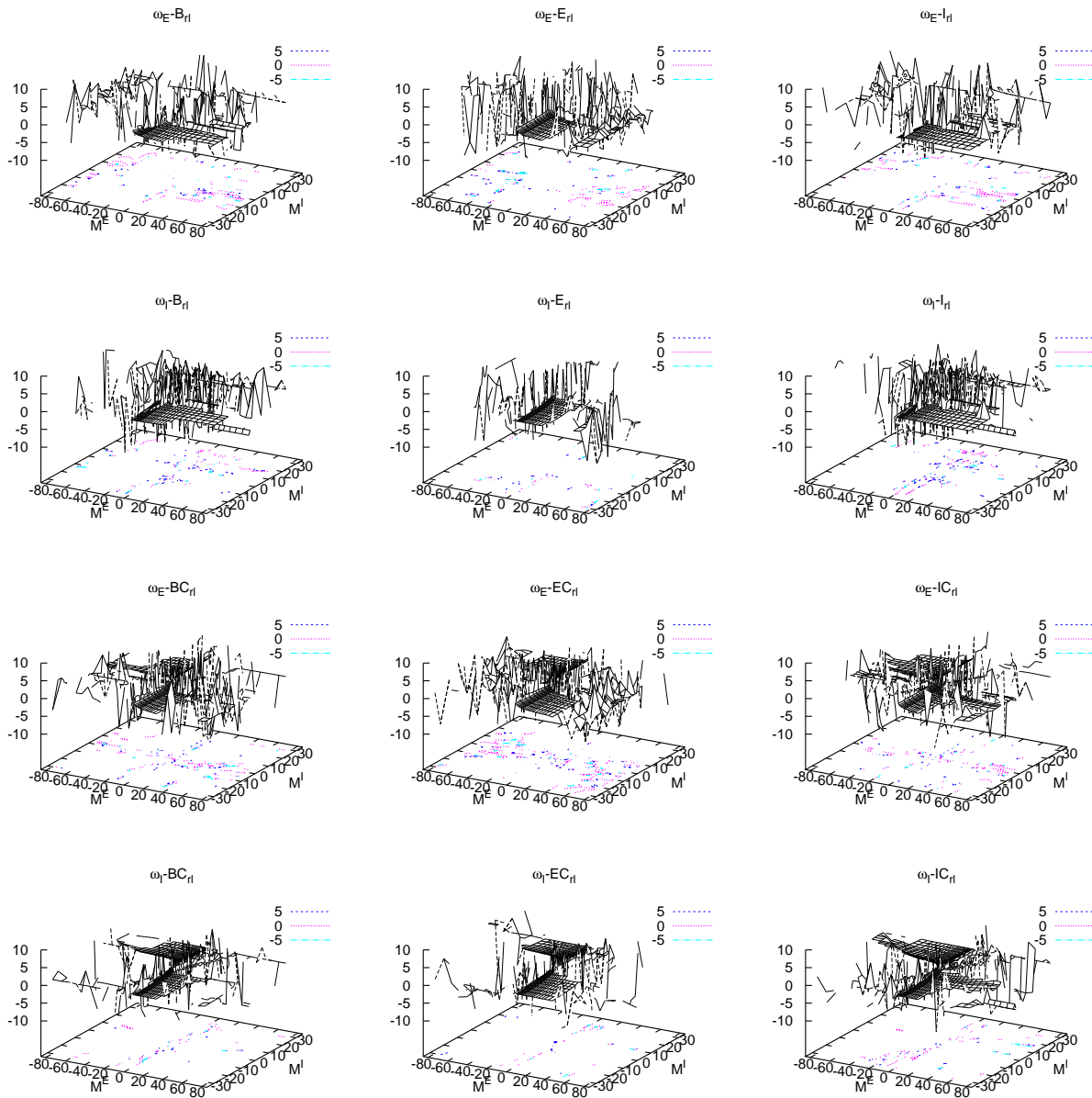
Fig. 14. Imaginary (attenuated) frequency solutions for Balanced, Excitatory and Inhibitory neocortical columnar firings, in columns 1-3 resp. Rows 3 and 4 are these cases with the centering mechanism. Solutions in rows 1 and 3 are ω_E, rows 2 and 4 are ω_I.
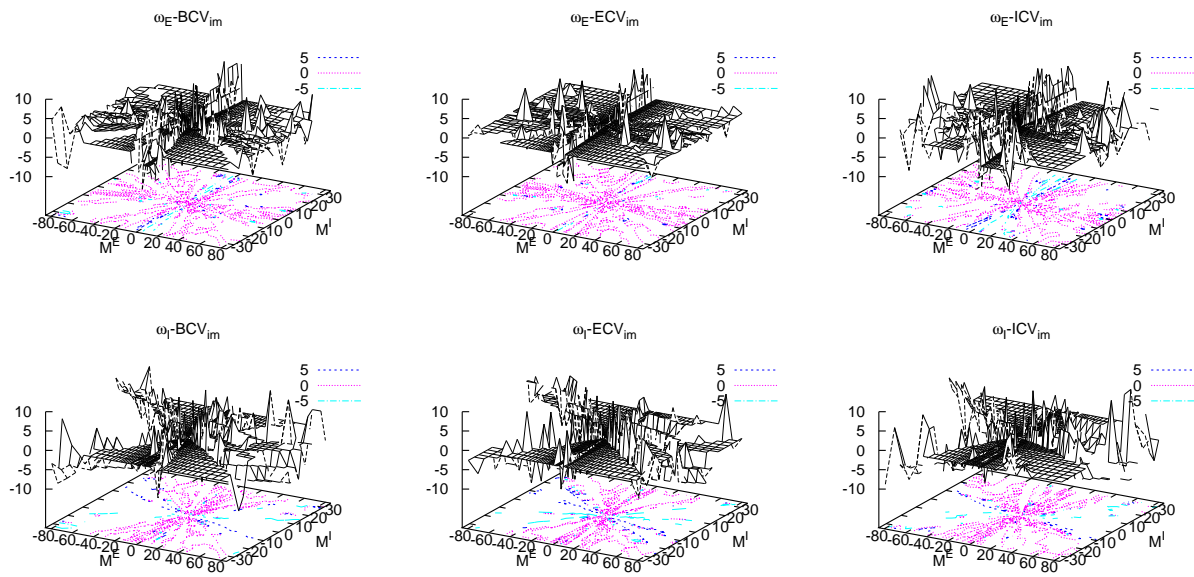
Fig. 15. Real (oscillatory) frequency solutions for Balanced, Excitatory and Inhibitory visual neocortical columnar firings, with the centering mechanism, in columns 1-3 resp. Solutions in row 1 are ω_E, row 2 are ω_I.
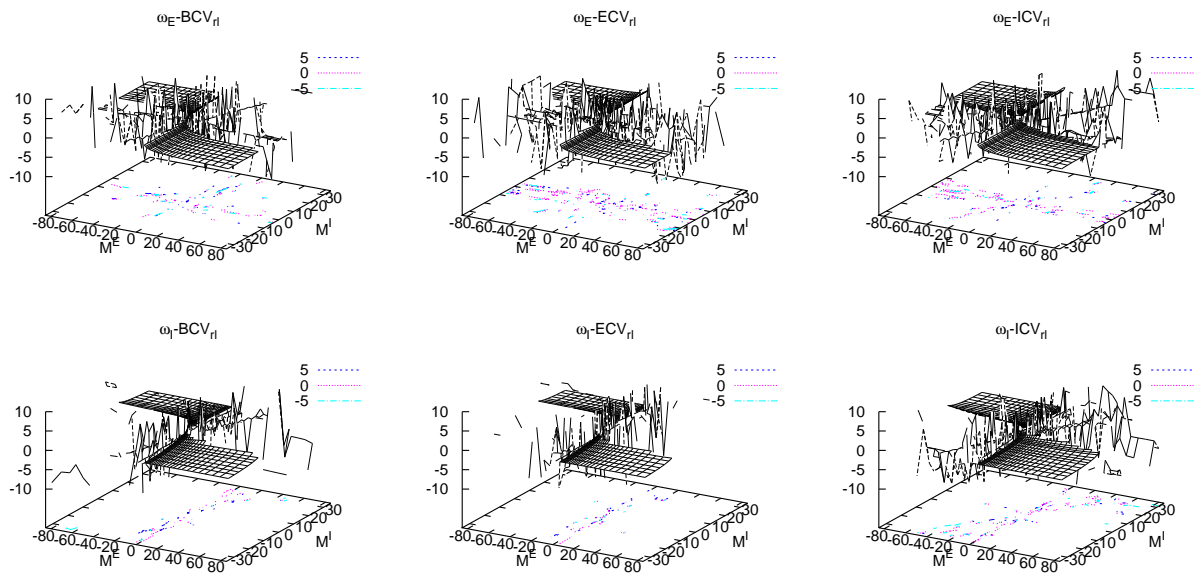
Fig. 16. Imaginary (attenuated) frequency solutions for Balanced, Excitatory and Inhibitory visual neocortical columnar firings, with the centering mechanism, in columns 1-3 resp. Solutions in row 1 are ω_E, row 2 are ω_I.
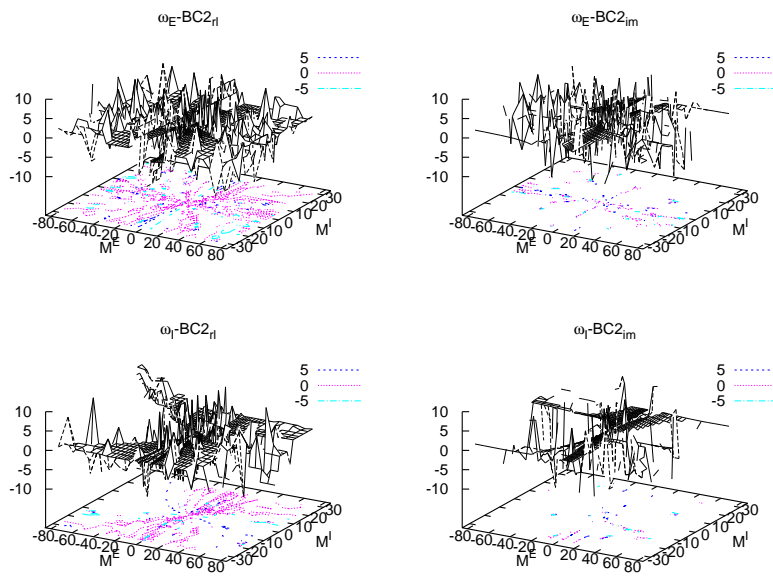
Fig. 17. For Balanced neocortical columnar firings with original $\sqrt{2}$ error, with the centering mechanism, real (oscillatory) frequency solutions are in column 1 and imaginary (attenuated) frequency solutions are in column 2. Solutions in row 1 are ω_E, row 2 are ω_I.

6. Conclusion on Conjecture of Neocortical Information Processing

It is reasonable to conjecture that if columnar firings of short-ranged fibers M^G can oscillate within harmonics of long-ranged fibers $M^{*\ddagger E}$, this could facilitate information processed at fine neuronal and synaptic scales to be carried across minicolumns and regional columns with relative efficiency. Note that this activity is at levels of 10^{-2} or 10^{-3} of the Lagrangian defining a small scale for STM, i.e., "zooming in" to still within classical (not quantum) domains of information.

While attractor states have been explicitly detailed in previous papers for several SMNI models, here oscillatory states have been calculated throughout the range of firing space. Clearly, oscillations within the columnar attractors should naturally have longer lifetimes, but given that long-ranged fiber interactions across regions can constrain columnar firings, it is useful to at least see how oscillations may be supported even in limited ranges of such constrained firings.

For example, during slow theta — often preset during sleep, during alpha — often present during "relaxed" attention, and during faster beta — often present during intense concentration, information inherent in dynamic STM firings as well as in relatively static synaptic parameters, are often merged into associative neocortex, and during conscious selective attention frontal cortex often controls processing of this information. The use of global carrier frequencies could aid in the noise suppression to convey this information.

Acknowledgments

REFERENCES

Graham, R. (1977) Covariant formulation of non-equilibrium statistical thermodynamics. Zeitschrift für Physik. B26, 397-405.

Ingber, L. (1981) Towards a unified brain theory. Journal Social Biological Structures. 4, 211-224. [URL http://www.ingber.com/smni81_unified.pdf]

Ingber, L. (1982) Statistical mechanics of neocortical interactions. I. Basic formulation. Physica D. 5, 83-107. [URL http://www.ingber.com/smni82_basic.pdf]

Ingber, L. (1983) Statistical mechanics of neocortical interactions. Dynamics of synaptic modification. Physical Review A. 28, 395-416. [URL http://www.ingber.com/smni83_dynamics.pdf]

Ingber, L. (1984) Statistical mechanics of neocortical interactions. Derivation of short-term-memory capacity. Physical Review A. 29, 3346-3358. [URL http://www.ingber.com/smni84_stm.pdf]

Ingber, L. (1985a) Statistical mechanics algorithm for response to targets (SMART), In: Workshop on Uncertainty and Probability in Artificial Intelligence: UC Los Angeles, 14-16 August 1985, American Association for Artificial Intelligence, 258-264. [URL http://www.ingber.com/combat85_smart.pdf]

Ingber, L. (1985b) Statistical mechanics of neocortical interactions. EEG dispersion relations. IEEE Transactions Biomedical Engineering. 32, 91-94. [URL http://www.ingber.com/smni85_eeg.pdf]

Ingber, L. (1985c) Statistical mechanics of neocortical interactions: Stability and duration of the 7+-2 rule of short-term-memory capacity. Physical Review A. 31, 1183-1186. [URL http://www.ingber.com/smni85_stm.pdf]

Ingber, L. (1986a) Riemannian contributions to short-ranged velocity-dependent nucleon-nucleon interactions. Physical Review D. 33, 3781-3784. [URL http://www.ingber.com/nuclear86_riemann.pdf]

Ingber, L. (1986b) Statistical mechanics of neocortical interactions. Bulletin American Physical Society. 31, 868.

Ingber, L. (1989) Very fast simulated re-annealing. Mathematical Computer Modelling. 12(8), 967-973. [URL http://www.ingber.com/asa89_vfsr.pdf]

Ingber, L. (1990) Statistical mechanical aids to calculating term structure models. Physical Review A. 42(12), 7057-7064. [URL http://www.ingber.com/markets90_interest.pdf]

Ingber, L. (1991) Statistical mechanics of neocortical interactions: A scaling paradigm applied to electroencephalography. Physical Review A. 44(6), 4017-4060. [URL http://www.ingber.com/smni91_eeg.pdf]

Ingber, L. (1992) Generic mesoscopic neural networks based on statistical mechanics of neocortical interactions. Physical Review A. 45(4), R2183-R2186. [URL http://www.ingber.com/smni92_mnn.pdf]

Ingber, L. (1993a) Adaptive Simulated Annealing (ASA). Global optimization C-code. Caltech Alumni Association. [URL http://www.ingber.com/#ASA-CODE]

Ingber, L. (1993b) Statistical mechanics of combat and extensions, In: Toward a Science of Command, Control, and Communications, ed. C. Jones. American Institute of Aeronautics and Astronautics, 117-149. [ISBN 1-56347-068-3. URL http://www.ingber.com/combat93_c3sci.pdf]

Ingber, L. (1994) Statistical mechanics of neocortical interactions: Path-integral evolution of short-term memory. Physical Review E. 49(5B), 4652-4664. [URL http://www.ingber.com/smni94_stm.pdf]

Ingber, L. (1995a) Statistical mechanics of multiple scales of neocortical interactions, In: Neocortical Dynamics and Human EEG Rhythms, ed. P.L. Nunez. Oxford University Press, 628-681. [ISBN 0-19-505728-7. URL http://www.ingber.com/smni95_scales.pdf]

Ingber, L. (1995b) Statistical mechanics of neocortical interactions: Constraints on 40 Hz models of short-term memory. Physical Review E. 52(4), 4561-4563. [URL http://www.ingber.com/smni95_stm40hz.pdf]

Ingber, L. (1996a) Nonlinear nonequilibrium nonquantum nonchaotic statistical mechanics of neocortical interactions. Behavioral and Brain Sciences. 19(2), 300-301. [Invited commentary on Dynamics of the brain at global and microscopic scales: Neural networks and the EEG, by J.J. Wright and D.T.J. Liley. URL http://www.ingber.com/smni96_nonlinear.pdf]

Ingber, L. (1996b) Statistical mechanics of neocortical interactions: Multiple scales of EEG, In: Frontier Science in EEG: Continuous Waveform Analysis (Electroencephalography Clinical Neurophysiology Suppl. 45), ed. R.M. Dasheiff & D.J. Vincent. Elsevier, 79-112. [Invited talk to Frontier Science in EEG Symposium, New Orleans, 9 Oct 1993. ISBN 0-444-82429-4. URL http://www.ingber.com/smni96_eeg.pdf]

Ingber, L. (1997) Statistical mechanics of neocortical interactions: Applications of canonical momenta indicators to electroencephalography. Physical Review E. 55(4), 4578-4593. [URL http://www.ingber.com/smni97_cmi.pdf]

Ingber, L. (1998) Statistical mechanics of neocortical interactions: Training and testing canonical momenta indicators of EEG. Mathematical Computer Modelling. 27(3), 33-64. [URL http://www.ingber.com/smni98_cmi_test.pdf]

Ingber, L. (2000) High-resolution path-integral development of financial options. Physica A. 283(3-4), 529-558. [URL http://www.ingber.com/markets00_highres.pdf]

Ingber, L. (2005) Trading in Risk Dimensions (TRD). Report 2005:TRD. Lester Ingber Research. [URL http://www.ingber.com/markets05_trd.pdf]

Ingber, L. (2006a) Ideas by statistical mechanics (ISM). Report 2006:ISM. Lester Ingber Research. [URL http://www.ingber.com/smni06_ism.pdf]

Ingber, L. (2006b) Statistical mechanics of neocortical interactions: Portfolio of physiological indicators. Report 2006:PPI. Lester Ingber Research. [URL http://www.ingber.com/smni06_ppi.pdf]

Ingber, L. (2007) Ideas by Statistical Mechanics (ISM). Journal Integrated Systems Design and Process Science. 11(3), 31-54. [Special Issue: Biologically Inspired Computing.]

Ingber, L. (2008) AI and Ideas by Statistical Mechanics (ISM), In: Encyclopedia of Artificial Intelligence, ed. J.R. Rabuñal, J. Dorado & A.P. Pazos. Information Science Reference, 58-64. [ISBN 978-1-59904-849-9]

Ingber, L. (2009) Statistical mechanics of neocortical interactions: Nonlinear columnar electroencephalography. NeuroQuantology Journal. 7(4), 500-529. [URL http://www.neuroquantology.com/journal/index.php/nq/article/view/365/385]

Ingber, L., Chen, C., Mondescu, R.P., Muzzall, D. & Renedo, M. (2001) Probability tree algorithm for general diffusion processes. Physical Review E. 64(5), 056702-056707. [URL http://www.ingber.com/path01_pathtree.pdf]

Ingber, L. & Nunez, P.L. (1990) Multiple scales of statistical physics of neocortex: Application to electroencephalography. Mathematical Computer Modelling. 13(7), 83-95.

Ingber, L. & Nunez, P.L. (1995) Statistical mechanics of neocortical interactions: High resolution path-integral calculation of short-term memory. Physical Review E. 51(5), 5074-5083. [URL http://www.ingber.com/smni95_stm.pdf]

Ingber, L., Srinivasan, R. & Nunez, P.L. (1996) Path-integral evolution of chaos embedded in noise: Duffing neocortical analog. Mathematical Computer Modelling. 23(3), 43-53. [URL http://www.ingber.com/path96_duffing.pdf]

Langouche, F., Roekaerts, D. & Tirapegui, E. (1982) Functional Integration and Semiclassical Expansions. Reidel, Dordrecht, The Netherlands.

Mountcastle, V.B. (1978) An organizing principle for cerebral function: The unit module and the distributed system, In: The Mindful Brain, ed. G.M. Edelman & V.B. Mountcastle. Massachusetts Institute of Technology, 7-50.

Mountcastle, V.B., Andersen, R.A. & Motter, B.C. (1981) The influence of attentive fixation upon the excitability of the light-sensitive neurons of the posterior parietal cortex. Journal of Neuroscience.

1, 1218-1235.

Nunez, P.L. (1974) The brain wave equation: A model for the EEG. Mathematical Bioscience. 21, 279-297.

Nunez, P.L. (1981) Electric Fields of the Brain: The Neurophysics of EEG. Oxford University Press, London.

Nunez, P.L. (1995) Neocortical Dynamics and Human EEG Rhythms. Oxford University Press, New York, NY.

Nunez, P.L. (2009) Brain, Mind, and the Structure of Reality. Oxford University Press, London.

Nunez, P.L. & Srinivasan, R. (1993) Implications of recording strategy for estimates of neocortical dynamics with electroencephalography. Chaos. 3(2), 257-266.

Nunez, P.L. & Srinivasan, R. (2006) Electric Fields of the Brain: The Neurophysics of EEG, 2nd Ed.. Oxford University Press, London.

Schelter, W. (2009) Maxima. DOE, http://maxima.sourceforge.net.

Srinivasan, R. & Nunez, P.L. (1993) Neocortical dynamics, EEG standing waves and chaos, In: Nonlinear Dynamical Analysis for the EEG, ed. B.H. Jansen & M. Brandt. World Scientific, 310-355.

Williams, T. & Kelley, C. (2008) Gnuplot. Dartmouth, http://gnuplot.sourceforge.net.

Zhou, C. & Kurths, J. (2003) Noise-induced synchronization and coherence resonance of a Hodgkin-Huxley model of thermally sensitive neurons. Chaos. 13, 401-409.